Aalto University
School of Engineering

Einari Heinaro

3D-Based Tree Detection in Urban Areas with Airborne Laser Scanning

Master's Thesis
Aalto University
School of Engineering
Department of Built Environment

Thesis submitted as a partial fulfilment of the requirements for the degree of Master of Science in Technology
Helsinki 18.11.2018
Supervisor: Prof. Matti Vaaja
Advisors: D.Sc. Petri Rönnholm
D.Sc. Topi Tanhuanpää

Aalto University
School of Engineering

Aalto University, P.O. BOX 11000, 00076
AALTO
www.aalto.fi

Abstract of master's thesis

Author Einari Heinaro

Title of thesis 3D-Based Tree Detection in Urban Areas with Airborne Laser Scanning

Master programme Geoinformatics **Code** ENG22

Thesis supervisor Prof. Matti Vaaja

Thesis advisor(s) D.Sc. Petri Rönnholm, D.Sc. Topi Tanhuanpää

Date 18.11.2018 **Number of pages** 60+2 **Language** English

Abstract

Urban trees are a valuable resource, as they affect the climate of cities, provide aesthetic and recreational value and maintain the biodiversity in the cities. Thus, cities and municipalities often keep tree registers for monitoring the condition of urban trees. Updating these registers with field measurements is laborious and time-consuming and thus there is a need to automate the updating process. Airborne laser scanning (ALS) provides an efficient option for the tree registry updating process, as it enables acquiring detailed three-dimensional (3D) data from large areas at once.

This thesis studied the ALS-based urban tree monitoring process starting from the extraction of vegetation points from the ALS point cloud and ending in the detection and delineation of individual trees. One method was developed and tested for removing falsely classified vegetation points from a pre-classified point cloud. In addition, three individual tree detection (ITD) methods were developed and tested. Method 1 detected trees using region growing, method 2 divided the point cloud into horizontal slices and delineated the trees by merging clusters of each slice, and method 3 detected trees from a surface model.

The method for removing falsely classified vegetation points produced varying results. Some false vegetation points originating from flat man-made objects were detected rather well, whereas the detection of vertical and narrow objects was very poor. In conclusion, the method by itself was not sufficient, but it could be used as a part of the vegetation point extraction process.

The accuracy of the ITD methods was assessed by calculating the tree detection rates with distance thresholds ranging from 0.5 m to 6 m. The distance threshold determined the maximum locational difference between a delineated tree and a reference tree for these trees to be matched. The detection rates of ITD methods 1,2 and 3 ranged from 0.09 to 0.79, 0.14 to 0.79 and 0.11 to 0.50, respectively. The study showed that none of the tested methods perform sufficiently well by themselves, but a combination of methods 1 and 3 could be a suitable method for detecting urban trees.

Keywords individual tree detection, laser scanning, airborne laser scanning, urban trees

Aalto-yliopisto
Insinööritieteiden
korkeakoulu

Aalto-yliopisto, PL 11000, 00076 AALTO
www.aalto.fi
Diplomityön tiivistelmä

Tekijä Einari Heinaro

Työn nimi 3D-Based Tree Detection in Urban Areas with Airborne Laser Scanning

Maisteriohjelma Geoinformatiikka **Koodi** ENG22

Työn valvoja Prof. Matti Vaaja

Työn ohjaaja(t) TkT Petri Rönnholm, MMT Topi Tanhuanpää

Päivämäärä 18.11.2018 **Sivumäärä** 60+2 **Kieli** englanti

Tiivistelmä

Kaupunkipuut ovat tärkeitä, sillä ne vaikuttavat kaupunkien ilmastoon ja biodiversiteettiin sekä tuottavat virkistysarvoa ja esteettistä arvoa. Tämän vuoksi monet kunnat ja kaupungit ylläpitävät puurekisteriä kaupunkipuiden kunnon valvomiseksi. Näitä rekistereitä päivitetään maastomittauksin, mikä on varsin työlästä ja näin ollen rekisterien päivittämistä pyritään automatisoimaan. Ilmalaserkeilaus mahdollistaa rekisterien tehokkaan päivittämisen, sillä ilmalaserkeilaamalla voi kerätä tarkkaa kolmiulotteista informaatiota laajoilta alueilta.

Tässä työssä tutustuttiin ilmalaserkeilaukseen perustuvaan kaupunkipuiden monitorointiin alkaen kasvillisuuspisteiden luokittelusta ja päättyen yksittäisten puiden tunnistukseen ja rajaamiseen. Esiluokitellussa pistepilvessä virheellisesti kasvillisuudeksi luokiteltujen laserpisteiden poistamiseksi kehitettiin menetelmä. Tämän lisäksi työssä tutkittiin kolmen yksinpuintulkintamenetelmän toimintaa kaupunkiympäristössä. Menetelmä 1 tunnisti puita alueen kasvatusta hyödyntämällä, menetelmä 2 jakoi laserpistepilven vaakasuoriin liuskoihin ja mallinsi puut yhdistelemällä kunkin liuskan klustereita ja menetelmä 3 tunnisti puita pintamallilta.

Virheellisesti kasvillisuuspiteiksi luokiteltujen laserpisteiden tunnistamiseen kehitetty menetelmä toimi vaihtelevasti. Tasapintaisista kohteista syntyneet laserpisteet tunnistettiin melko hyvin, mutta kapeat ja pystysuorat kohteet tunnistettiin varsin huonosti. Näin ollen menetelmä ei yksinään ole riittävä virheellisten kasvillisuuspisteiden poistamiseen, mutta sitä voisi käyttää osana kasvillisuuspisteiden luokitteluprosessia.

Yksinpuintulkintamenetelmien tarkkuutta mitattiin laskemalla puiden tunnistusaste, eli kuinka suuri osa koealueiden puista kyettiin tunnistamaan kullakin menetelmällä. Referenssipuun ja yksinpuintulkintamenetelmällä mallinnetun puun yhdistämiseen käytettiin etäisyyden kynnysarvoja, jotka vaihtelivat 0,5 metristä 6 metriin. Menetelmien 1, 2 ja 3 tunnistusasteet vaihtelivat välillä 0,09-0,79, 0,14-0,79 ja 0,11-0,50. Tutkimus osoitti, että yksikään menetelmistä ei yksinään toimi riittävän hyvin. Sen sijaan menetelmien 1 ja 3 yhdistelmä voisi olla sopiva menetelmä kaupunkipuiden yksinpuintulkintaan.

Avainsanat yksinpuintulkinta, laserkeilaus, ilmalaserkeilaus, kaupunkipuut

Acknowledgements

Last winter I was considering a suitable and interesting subject for my master's thesis. I came to the conclusion that I wanted the subject to be somehow related to forests which are an important and familiar place for me through my hobby – orienteering. I ended up contacting the Department of Forest Sciences of the University of Helsinki and after a while of discussion, my thesis topic was agreed upon.

I would like to thank Matti Vaaja for supervising my thesis. In addition, I would like to express my deepest gratitude to my advisors Topi Tanhuanpää and Petri Rönnholm for guiding me through the thesis writing process and giving valuable feedback. Furthermore, I am grateful to Markus Holopainen from the University of Helsinki for helping me find an interesting topic. Finally, a big thank you to my parents for their support during the thesis writing process.

Helsinki 18.11.2018

Einari Heinaro

Table of contents

Abbreviations

2D	Two-Dimensional
3D	Three-Dimensional
ALS	Airborne Laser Scanning
ASPRS	American Society for Photogrammetry and Remote Sensing
CHM	Canopy Height Model
CMM	Canopy Maxima Model
DBH	Diameter at Breast Height
DGNSS	Differential Global Navigation Satellite System
DTM	Digital Terrain Model
DSM	Digital Surface Model
FOV	Field of View
GNSS	Global Navigation Satellite System
IFOV	Instantaneous Field of View
ITD	Individual Tree Detection
IMU	Inertial Measurement Unit
LASER	Light Amplification by Stimulated Emission of Radiation
LiDAR	Light Detection and Ranging
MLS	Mobile Laser Scanning
NDVI	Normalised Difference Vegetation Index
POS	Position and Orientation System
PRF	Pulse Repetition Frequency
TLS	Terrestrial Laser Scanning
UAV	Unmanned Aerial Vehicle
VHR	Very High Resolution

1 Introduction

1.1 Background

Urban trees have several purposes. They affect the air quality and temperature of cities, provide homes for many species and provide recreational value (Konijnendijk et al. 2005). The growing conditions of urban trees are, however, often rather challenging, as they must live within man-made environments where water and soil resources are scarce. Thus, urban trees must be maintained to ensure their wellbeing. The maintenance of urban trees is laborious and expensive and thus must be focused on the trees with most urgent needs. Monitoring urban trees provides valuable information of tree conditions. This information can be used for deciding which trees require maintenance. For this reason, many cities have a tree register, which is regularly updated (Tanhuanpää et al. 2014).

Urban trees have traditionally been monitored with field measurements (Tanhuanpää 2016). Field monitoring has included visual inspection and measuring descriptive tree attributes such as diameter at breast height (DBH) and tree height (Nielsen et al. 2014). Field measurements are, however, rather slow and laborious (Nielsen et al. 2014) and thus there is a need for a more efficient and automated method for urban tree monitoring.

Remote sensing has been used for non-urban forest inventory for several decades, as it provides an efficient and mostly automated way of mapping and monitoring large areas at once. Similar methods have been used for urban forest inventory with varying results. So far, the remote sensing methods used have mainly been photogrammetric and only a few methods have been developed for urban tree monitoring with airborne laser scanning (ALS) (Nielsen et al. 2014). However, laser scanners have one major advantage compared to photogrammetric methods, as they can penetrate the top-most layer of tree crowns thus providing 3D information of trees. Thus, ALS has considerable potential in urban tree monitoring.

1.2 Study objectives

This study examines the suitability of airborne laser scanning for the detection of trees in urban areas. The process of urban tree detection consists of two steps: separating vegetation points from the points of other objects in the laser point cloud and detecting and delineating individual trees from the separated vegetation points. The first of these two steps can be further divided into creating a preliminary classification of the point cloud and improving the vegetation point classification. This study tries to answer the following two research questions:

1. How can the classification of vegetation points be improved?
2. Which ALS-based method is the most effective in detecting individual trees in urban areas?

Both research questions are answered by testing algorithms and methods and assessing their performance. The methods are tested on an ALS dataset acquired from the city of Helsinki with an Optech Titan multispectral laser scanner in the summer of 2017.

1.3 Research limitations

1.3.1 Vegetation point extraction

Extracting vegetation points from a laser point cloud can be divided into creating a preliminary classification and improving the vegetation point classification. The preliminary classification step includes separating ground points from other laser points and classifying the above-ground points into classes such as buildings, low vegetation and high vegetation. Improving the vegetation point classification, in turn, includes separating real vegetation points from the falsely classified vegetation points. The empirical part of this study focuses mostly on this second step of vegetation point extraction.

1.3.2 Individual tree detection

This study focuses on ALS-based individual tree detection methods. Other tree detection methods, such as photogrammetric methods, terrestrial laser scanning (TLS) and mobile laser scanning (MLS) are mentioned briefly, but they are not included in the empirical part of this study. ALS methods using unmanned aerial vehicles (UAVs) are also excluded from this study. Furthermore, other ALS-based tree inventory methods, such as area-based methods are briefly described, but the focus is mainly on individual tree detection.

The emphasis of this study is on urban trees. However, the methods presented in the study have mostly been designed for and tested in non-urban forests, as not many purely ALS-based urban tree detection methods have yet been created. The idea is to test, whether some of these individual tree detection methods would be suitable for urban environments. Furthermore, only 3D-based individual tree detection methods (i.e., methods using the whole laser point cloud) are tested in the empirical part of this study, as these methods have more potential in detecting and delineating individual trees accurately than methods using surface models created from the point cloud.

This study addresses only the detection and delineation of individual trees. The purpose of tree detection and delineation is to enable the estimation of tree attributes, such as DBH and tree species. However, only one directly measurable tree attribute – the tree height – is used in assessing the performance of the methods. Further tree attribute estimation is beyond the scope of this study.

1.4 Thesis structure

The structure of this thesis goes as follows. Chapters 2 to 5 provide a literature review of the relevant concepts and methods of this study. Chapter 2 presents the basic theory of laser scanning and introduces the various types of laser scanning and laser scanners. Chapter 3 discusses the purpose of urban tree monitoring, presents the urban tree types and describes how urban trees are mapped. Chapter 4 presents methods for the extraction of vegetation points from the laser point cloud. Chapter 5 describes the process of measuring tree attributes and presents methods for individual tree detection and delineation.

Chapters 6 to 8 discuss the empirical part of this study. Chapter 6 presents the data and methods used in this study, chapter 7 presents the results of the study and chapter 8 discusses the results. Finally, the study is concluded in chapter 9.

2 Laser scanning

Laser (Light Amplification by Stimulated Emission of Radiation) is, in its simplest terms, amplified light that is used for a wide range of purpose (Milonni & Eberly 2010). Laser scanners are active instruments used for measuring the 3D-characteristics of objects and targets remotely. The applications of laser scanning range from the microscopic scale (Denk et al. 1990) to a nation-wide scale (Oksanen 2012). Laser scanners are gaining popularity in forest and tree monitoring, as they enable acquiring accurate 3D data from the forests (Holopainen et al. 2013a).

The following chapters will provide an introduction to laser scanning. Chapter 2.1 presents the various types of laser scanning used for forest and tree inventory. Chapter 2.2 introduces the basic principles of ALS, the most central laser scanning method to this study. Chapter 2.3 discusses the two types of laser scanners: discrete and full-waveform laser scanners. The last chapter presents multispectral laser scanning - laser scanning that provides spectral information from the measurable object/target in addition to the 3D information.

2.1 Types of laser scanning

Three types of laser scanning are used for forest and tree inventory: ALS (airborne laser scanning), TLS (terrestrial laser scanning) and MLS (mobile laser scanning) (Holopainen et al. 2013a). These methods differ from each other in the way they acquire 3D information from the target. ALS scans the target from above (i.e., from the air), whereas TLS and MLS are ground-based methods. TLS scans the target from stationary measuring points, whereas MLS acquires 3D information from a moving platform.

Airborne laser scanners are mounted on an aerial vehicle, such as an airplane or helicopter (Figure 1). More recently, laser scanners have also been mounted on UAVs (unmanned aerial vehicles) (Jaakkola et al. 2010, Wallace et al. 2014). So far, airplanes have remained the most frequently used platforms in ALS-based forest inventory, but UAVs are gaining more interest in several small-scale applications, as they are able to provide data of very high resolution (Jaakkola et al. 2010). ALS methods acquire 3D information by scanning the target area while flying over the area. The flying altitude of conventional ALS platforms ranges from several hundreds of metres to several kilometres (Holopainen et al. 2013a), whereas the flying altitude of UAVs is some tens of metres (Jaakkola et al. 2010). Thus, one major advantage of ALS is that it can acquire information from large areas at once. ALS methods typically collect data by flying several times over the monitorable area in parallel and perpendicular flight lines. This ensures the comprehensiveness and quality of the data (Holopainen et al. 2013a). The point density of ALS ranges from 0.5 laser points/m^2 up to 50 laser points/m^2 (Holopainen et al. 2013a). A more detailed description of the ALS methodology is presented in the next chapter.

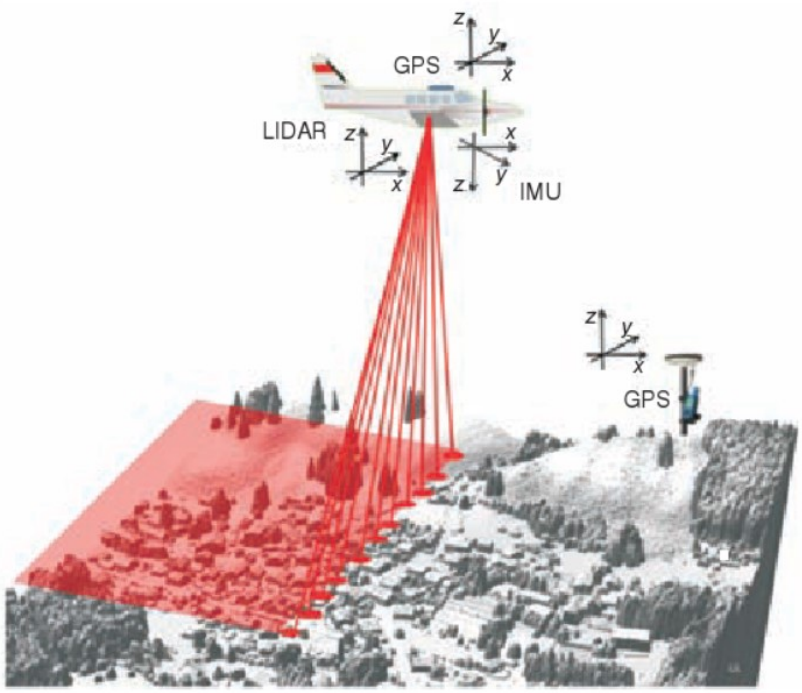

Figure 1 Airborne laser scanning (Vosselman & Maas 2010)

Terrestrial laser scanning is a ground-based method for acquiring 3D information of targets. TLS can provide very high-resolution information (tens of thousands of laser points per square metre) of the measurable target. However, TLS is only suitable for measuring rather small areas, as the method is stationary and the distance to the target is very short. In TLS, a laser scanner is set on top of a tripod (Figure 2). The scanner measures the range and direction to the target. When the accurate position of the scanner is known, each measurement can be converted to a 3D point. The problem with a single measurement position is that some objects cannot be measured, as they are behind other objects. Thus, the target area is often measured from several different directions and the measurements acquired from each direction are combined afterwards. (Holopainen et al. 2013a.)

Figure 2 A terrestrial laser scanner (Holopainen et al. 2013a, ©Ville Kankare)

Mobile laser scanners measure the target from a ground-based moving platform, such as a car (Figure 3) or a motorcycle. In some cases, mobile laser scanners have even been mounted on a backpack (Kukko et al. 2012). The data collection method of MLS is similar to the one of TLS: the scanner measures directions and ranges to the target and when the position of the scanner is known, each measurement can be converted to a 3D point. However, the moving platform sets different requirements for data processing, as the position of the scanner changes continuously. MLS provides an efficient way of collecting high-accuracy 3D information (several hundreds of laser points per square metre) of targets, as the distance to the target is rather short, but the data collection is fast. In some cases, MLS provides a viable option for ALS, as the data accuracy is higher, but the data can still be collected rather efficiently. MLS is especially useful in urban areas where the road network is dense. However, the applications of MLS are limited, as cars and motorcycles cannot access areas without roads. One solution to this problem is the use of UAVs as platforms, as they do not depend on roads. Laser scanning with UAVs was already introduced as an ALS method. However, it can be seen either as an ALS method or an MLS method depending on the application. (Holopainen et al. 2013a, Holopainen et al. 2013b.)

Figure 3 A mobile laser scanner on top of a car (Holopainen et al. 2013a, ©Antero Kukko)

2.2 Principles of airborne laser scanning

The term ALS is often used interchangeably with another term: LiDAR (Light Detection and Ranging). However, LiDAR is a wider term for airborne laser-based methods, as in addition to ALS, it includes laser profiling. The difference between ALS and laser profiling is that laser profiling only measures the target directly below the flight line, whereas ALS scans a wider area at once. (Holopainen et al. 2013a.)

The basic idea of ALS is fairly simple. The target is measured by flying over it in several flight lines. The laser scanner mounted on an aerial vehicle sends laser pulses to the target and measures the time delay of the returning echoes. These time measurements can be converted to range measurements with the following equation:

$$R = \frac{ct}{2}, \tag{1}$$

where R is the range to the target, c is the speed of light and t is the time delay between the sent and received laser pulse. Equation 1 has a denominator of 2, as the range to the target is only half of the total distance the laser pulse travels. The direction of the sent pulses is changed, so that a wider area can be measured on a single flight line. When the accurate position and orientation of the laser scanner is known at each point in time, the range measurements can be converted to 3D coordinates. (Wehr & Lohr 1999, Baltsavias 1999, Holopainen et al. 2013a.) Figure 4 presents the basic idea of ALS.

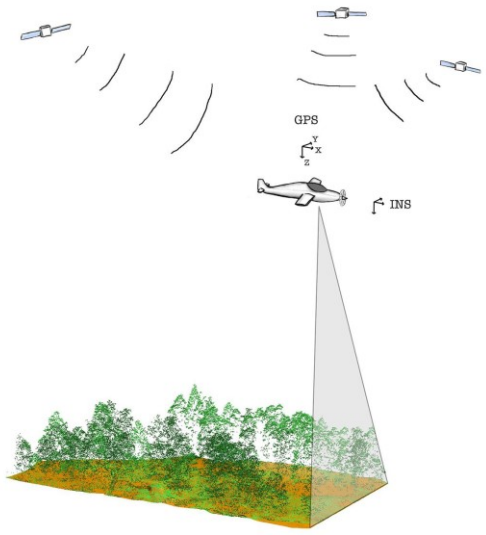

Figure 4 Airborne laser scanning (Holopainen et al. 2013a, ©Ville Kankare)

2.2.1 Components of an airborne laser scanning system

An ALS system contains the following components: a laser ranging unit, an opto-mechanical scanner, and a position and orientation system (Figure 5). The purpose of the laser ranging unit is to create laser pulses or continuous waves and measure their travelling time. Thus, the laser ranging unit contains a laser and a receiver. The laser emits pulses or continuous waves and their echoes are captured by the receiver. Both the laser transmitter and receiver share the same optics, which ensures that the echo of an emitted laser pulse is always visible for the receiver. (Wehr & Lohr 1999.)

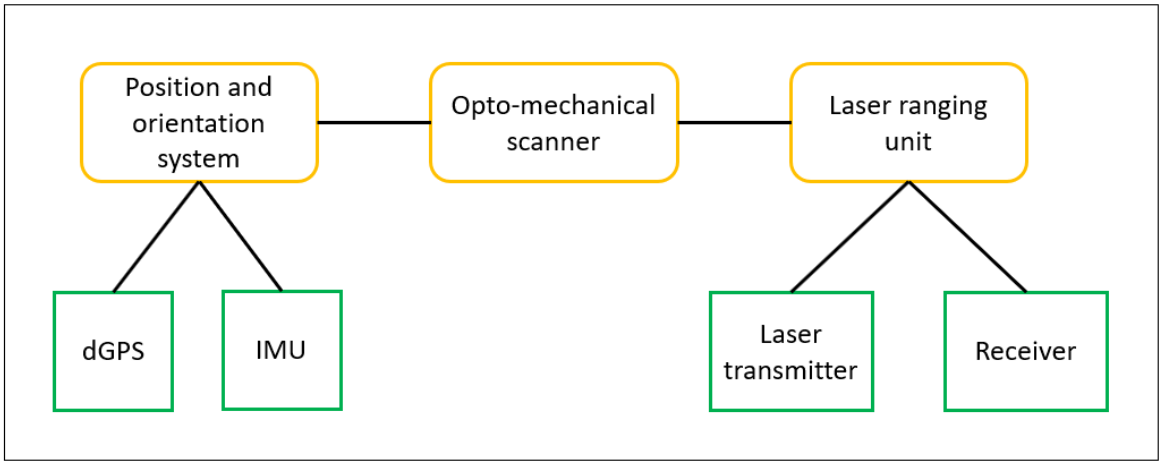

Figure 5 The components of an airborne laser scanner

The opto-mechanical scanner controls the direction in which the laser pulses are sent. Thus, it provides the laser scanner with its scanning ability. The opto-mechanical scanner directs the laser pulses with moving mirrors and, in some cases, optical fibres. Different scanners produce different scanning patterns, such as an elliptical pattern (Figure 6, left) or a line-like pattern (Figure 6, centre and right). The pattern can be unidirectional (Figure 6, right), meaning that the scanning is only done in one direction (e.g. left to right), or bidirectional (Figure 6, centre), meaning that the scanning is done in both directions. Note that in both

cases the scanning patterns are not exactly parallel to the flight direction, as the scanning is done from a moving platform. In addition, the patterns are not as uniform as shown in the figure, as the direction and velocity of the platform might vary. (Wehr & Lohr 1999.)

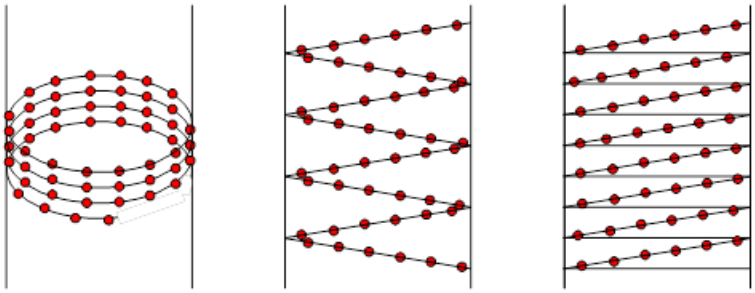

Figure 6 Different scanning patterns: an elliptical scan, a bidirectional line scan and a unidirectional line scan (Holopainen et al. 2013a)

The position and orientation system (POS) consists of two components (Figure 5): a global navigation satellite system (GNSS) and an inertial measurement unit (IMU). The GNSS measures the location of the laser scanner at each moment, whereas the IMU measures the orientation. Usually a differential GNSS (DGNSS) is used, as the accuracy of a regular GNSS device is not sufficient. A DGNSS uses ground reference stations to improve accuracy. The accurate position and orientation measurements of the POS enable converting the range measurements to 3D coordinates. However, the clocks of the laser scanner, GNSS and IMU must be synchronised accurately, so that the corresponding measurements can be identified from each device. (Vosselman & Maas 2010, Wehr & Lohr 1999.)

2.2.2 Pulse-based and continuous-wave laser scanners

Laser scanners can be divided into two groups: pulse-based and continuous wave (phase-based) laser scanners. These two groups differ from each other in the method they use for measuring the range to the target. The more frequently used pulse-based laser scanners send short, high-intensity laser pulses to the target and measure the time it takes for their echoes to return to the receiver. The time can then be converted to a range measurement with equation 1. (Wehr & Lohr 1999.)

Continuous wave laser scanners, in turn, send continuous, phase-modulated laser light to the target and calculate the range from the phase shift between the sent and received laser signals. The modulation is often performed to the intensity of the laser light, so that, for example, the intensity varies sinusoidally. When the period of the modulated signal is known, the range can be calculated from the travelling time of the signal. The following equation presents the relation between the travelling time of the laser signal, and the phase shift between the sent and received signals:

$$t = \frac{\phi}{2\pi}T + nT. \qquad (2)$$

In equation 2, t is the travelling time of the laser signal, ϕ is the phase difference between the sent and received signals, T is the period of the modulated signal and n is the number of full periods. Simply put, the travelling time of the laser signal is equal to the total number of periods the laser signal travels plus the time it takes in the phase shift. Equation 2 can be inserted to equation 1 to get the range equation for the phase-modulated signal:

$$R = \frac{cT}{2}\left(\frac{\phi}{2\pi} + n\right). \quad (3)$$

Equation 3 can be further modified to the following form:

$$R = \frac{\lambda}{2}\left(\frac{\phi}{2\pi} + n\right), \quad (4)$$

as the wavelength λ of the modulated signal is equal to the velocity of the signal (c) times the period (T). (Wehr & Lohr 1999.)

2.2.3 Parameters of airborne laser scanning

The following list presents some important parameters of ALS:

- flying height
- flying speed
- overlap of adjacent flight lines
- wavelength
- laser footprint
- scanning angle
- swath width
- point density
- pulse repetition frequency (PRF)

Each of these parameters either describes or affects the accuracy and properties of the acquired ALS data. Thus, the parameters should be chosen so that they best suit the application.

The flying height and speed both affect the accuracy of the acquired data. A low flying height and speed allow acquiring accurate data but require a more time-consuming data acquisition process. Similarly, a larger overlap of adjacent flight lines improves the data accuracy and reliability but requires a larger number of flight lines to be flown. Thus, choosing the flight parameters is always a compromise between the data accuracy, time and cost. (Vosselman & Maas 2010, Holopainen et al. 2013a.)

The laser wavelength has an impact on what kind of information can be acquired from the target. The reflectance of different objects varies depending on the wavelength. Thus, the laser wavelength should be chosen so that it maximises the reflectance of the objects of interest. (Vosselman & Maas 2010.)

The laser footprint (Figure 7, right) is the spot on the target that one laser pulse illuminates. Its size is described with its diameter. The size of the laser footprint determines how small details can be identified from the object. The size of the laser footprint is determined by the flying height and the divergence of the laser beam. (Vosselman & Maas 2010.)

The scanning angle is the angle between the direction in which the laser pulse is emitted and the nadir (i.e., the direction directly below the laser scanner). A large maximum scanning angle allows scanning a wider area on a single flight line. However, the accuracy of the data decreases as the scanning angle increases. The metric counterpart of the scanning angle is called the swath width (Figure 7, left). It describes the width of the area that can be measured on a single flight line. (Vosselman & Maas 2010, Wehr & Lohr 1999.)

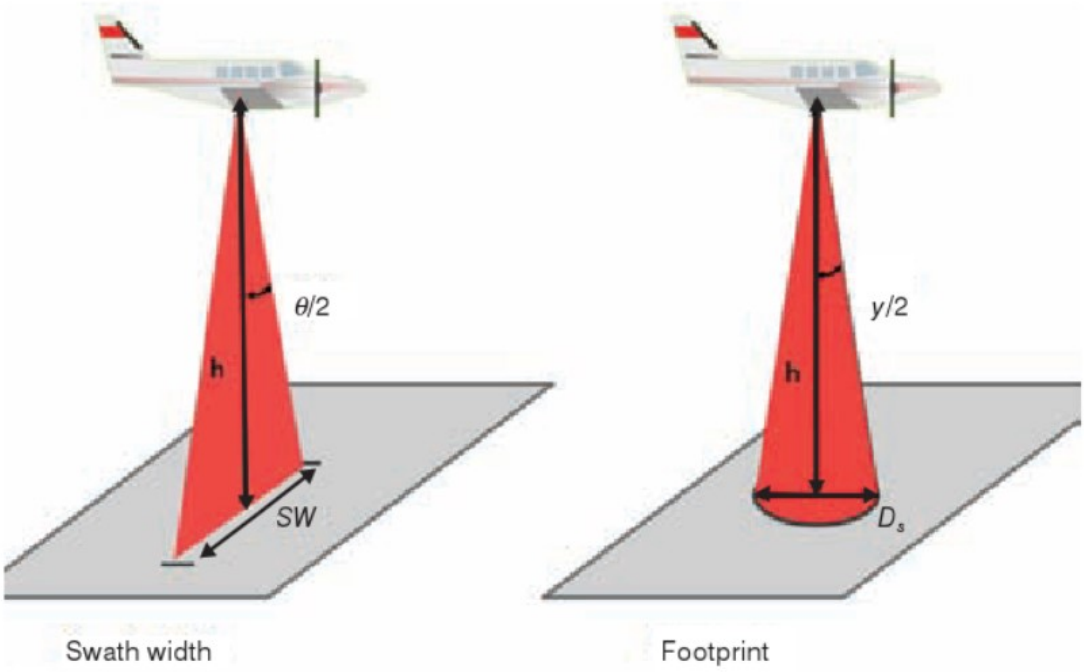

Figure 7 The swath width and the laser footprint. SW denotes the swath width, h the flying height, θ the scanning angle, D_s the diameter of the footprint and y the beam divergence. (Vosselman & Maas 2010)

The point density of the laser data is measured as points per square metre. It determines what kind of information can be acquired from the laser data. A high point density enables detailed analysis of individual objects, such as trees, whereas a low point density constrains the analysis to a larger scale. The point density is affected by other parameters, such as the pulse repetition frequency (PRF), scanning angle, overlap of adjacent flight lines, and the height and speed of the ALS platform. (Holopainen et al. 2013a, Vosselman & Maas 2010.)

The pulse repetition frequency (PRF) describes the frequency in which the laser can emit laser pulses. It is measured as pulses per second (i.e., Hertz). The PRF strongly affects the point density of the laser data. (Vosselman & Maas 2010, Wehr & Lohr 1999.)

2.3 Discrete and full-waveform laser scanners

The laser footprint is often much larger than the smallest detail of the target. Thus, when a laser signal hits an object, only a portion of it reflects from the top-most part of the object and the rest continues further until it reflects from deeper layers of the object. Thus, a single emitted laser signal produces multiple returns. There are two types of laser scanners: ones that detect only the intensity peaks of the returning signal and ones that capture the whole returning signal. These laser scanners are called discrete and full waveform laser scanners, respectively (e.g. Vosselman & Maas 2010). All continuous-waveform laser scanners are discrete scanners, whereas pulse-based laser scanners can be either discrete or full-waveform scanners.

Discrete laser scanners detect a laser return when its intensity is larger than a certain threshold (Figure 8a). A discrete laser scanner can detect up to five returns of a single signal.

However, the simplest discrete scanners only detect the first and last return of the signal. These returns correspond to the reflections of the top-most part of the target and the ground. Discrete scanners have a short dead time after detecting a return and thus they cannot detect intensity peaks that are too close to each other. This limits the resolution of the scanners. (Vosselman & Maas 2010, Lindberg et al. 2014.)

Full-waveform laser scanners record the whole returning signal. This means that, in contrast to discrete scanners, full-waveform scanners can detect the returning signal even if the intensity of the signal is rather low. Figure 8b depicts the full waveform of a returning laser signal reflected from a tree. Figure 8c shows how the full-waveform scanner measures the returning signal: as discrete returns with a very frequent measuring interval. Thus, practically the full-waveform scanner is able to capture even the slightest details of the returning signal. (Vosselman & Maas 2010.) This allows full-waveform scanners to acquire higher point density data from the target compared to discrete scanners (Reitberger et al. 2009).

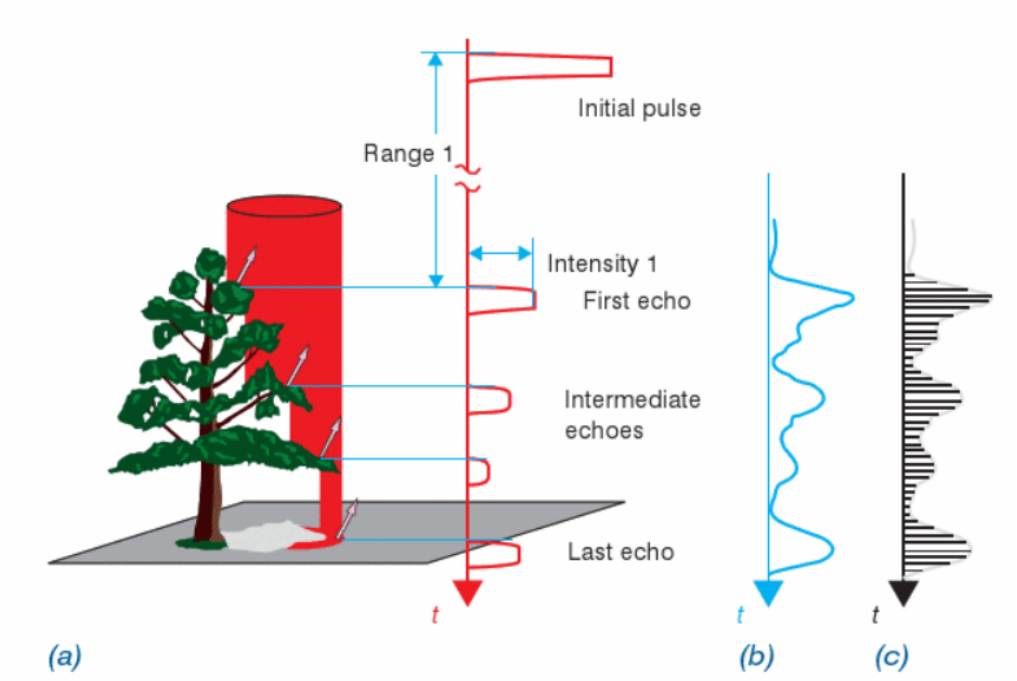

Figure 8 a) The returns of a discrete laser scanner b) The full waveform of the returning signal c) The digitised full waveform of the returning signal. (Vosselman & Maas 2010.)

2.4 Multispectral laser scanning

Conventionally, laser scanners have emitted laser light of just one wavelength. Different targets reflect the various wavelengths of light in different ways and thus the most suitable laser scanner has been chosen based on the reflective properties of the monitorable target. Spectral information combined with laser scanning data can allow a more detailed and accurate interpretation of the data (Budei et al. 2018). Thus, in some cases, aerial images have been combined with laser scanning data (e.g. Lang et al. 2006). In addition, multispectral laser scanning data have been acquired by combining scanning data of laser scanners with different wavelengths (e.g. Lindberg et al. 2015).

The first multispectral airborne laser scanner, the Optech Titan, was introduced in 2014. The scanner emits laser light of three different wavelengths and is thus suitable for several

applications. The wavelengths that Titan uses are 532 nm, 1064 nm and 1550 nm, which fall within the visible spectrum, the near infrared spectrum and the intermediate infrared spectrum respectively (Teledyne Optech 2015) (Figure 9). According to Teledyne Optech (2015), the benefits of their scanner include the possibility to acquire multispectral information regardless of the weather or time of day, and the possibility to use the spectral data to better differentiate the different objects and materials from each other.

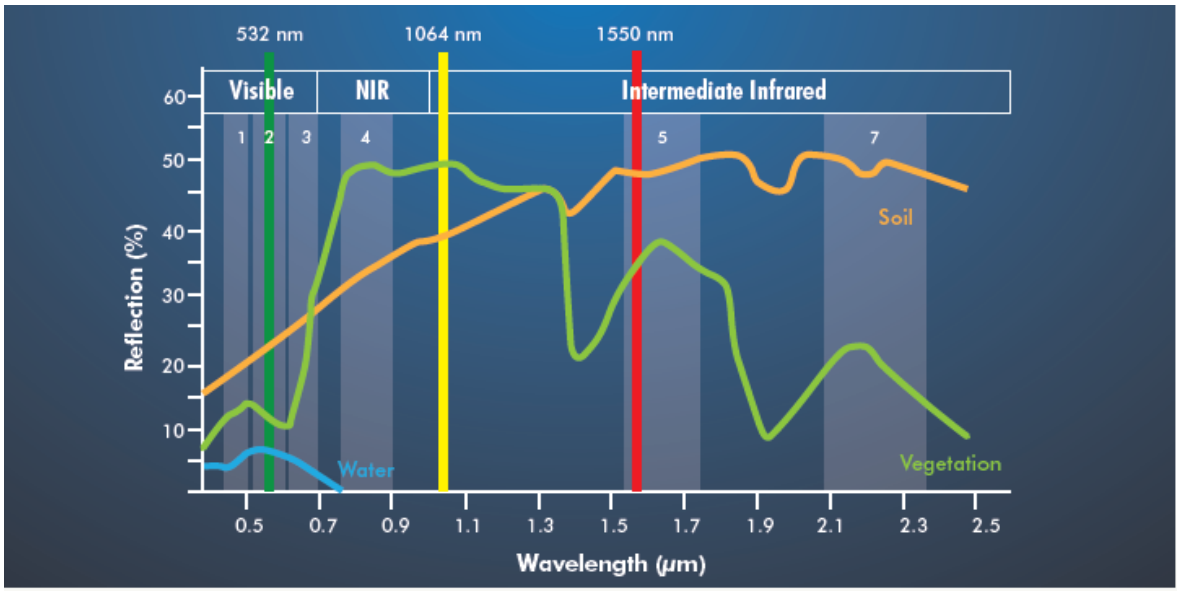

Figure 9 The laser wavelengths of the Optech Titan laser scanner (Teledyne Optech 2015)

3 Urban trees

The trees growing within or close to human settlements are called urban trees. They are needed for several purposes. Urban trees affect the air and climate of cities, provide recreational and aesthetic value and help to maintain the biodiversity in the cities (Tanhuanpää 2016, Bolund & Hunhammar 1999). However, urban trees require intensive management and care, as their growing conditions are often challenging. Urban tree monitoring provides information of the tree conditions and thus enables focusing the limited caretaking resources to the trees that require them the most.

The following chapters will address urban trees and their monitoring in more detail. The first chapter will present the types of urban trees. The second chapter will discuss the purpose of urban tree monitoring. The third chapter will discuss the ways in which urban trees are mapped and monitored.

3.1 Types of urban trees

Urban trees can be classified based on where they grow. Tanhuanpää (2016) divided urban trees into four different classes. The first class consists of roadside trees or street trees that are in the immediate vicinity of roads and streets. Street trees can grow either beside or in between roads. The second class consists of yard trees that belong to private properties. The third class are park trees that grow in managed parks. The fourth class consists of trees located in recreational forests, which are forests with a dense trail network.

The various types of urban trees are managed in different ways. Roadside trees, street trees and park trees are managed intensively, as trees of these types can present hazards if left unmaintained. Yard trees are often also maintained rather intensively, but in most cases, they are maintained by the property owner. Conversely, recreational forests often receive minimal maintenance and are mostly left in their natural state. For example, maintenance of recreational forests might only consist of clearing fallen trees that are blocking a trail. (Tanhuanpää 2016.)

3.2 Purpose of urban tree monitoring

Urban trees and forests have various ecological, social, economic, safety and health effects on their surroundings. Many of these effects are positive, but also some negative effects can be identified. These positive and negative effects are often called ecosystem services and disservices (e.g. Daily 1997, Lyytimäki et al. 2008). From the ecological perspective, urban trees and forests have mostly positive effects, such as improving urban air quality (Nowak et al. 2006) and regulating the local climate (Bolund & Hunhammar 1999). According to Bolund et al. (1999) urban trees also help to regulate the flow of rainwater and reduce noise from nearby traffic. Furthermore, urban trees and forests enable various recreational activities and provide aesthetical value. However, according to Lyytimäki et al. (2008) some ecological disservices of urban trees and forests include health issues caused by pollen, safety issues caused by fallen trees and dark parks, and aesthetical issues concerning unmaintained urban forests.

Urban trees are monitored to increase the value they provide. Thus, monitoring urban trees aims in finding ways that maximise the amount of ecological services and minimise the amount of ecological disservices urban trees provide. Various groups, from which city

authorities, residents and researchers are possibly the most remarkable, all have their own interests in urban trees. Researchers are largely interested in how urban trees affect their surroundings and, conversely, how the urban environment affects the trees (Nielsen et al. 2014). City authorities are more interested in practical applications of urban tree data. Monitoring urban trees allows them to make decisions on the maintenance of trees. For example, city authorities might decide whether a tree requires pruning or external protection based on tree condition data (Tanhuanpää 2016). Moreover, monitoring street trees and trees close to buildings enables taking reactive measures when a potentially hazardous tree is identified (Keller & Konijnendijk 2012). For these particular reasons, many cities have a tree register, which is used for monitoring the changes in tree conditions (Tanhuanpää et al. 2014). The relevancy and usefulness of the tree register depends on how often it is updated. Thus, efficient methods for updating the tree register are required.

3.3 Urban tree mapping

Urban trees have been mapped and monitored with several methods. One thing common to most of these methods is that they map urban trees on a single tree level, as most uses of urban tree data require data of this level (Nielsen et al. 2014). Nielsen et al. (2014) studied the various urban tree inventory methods by reviewing the urban tree-related scientific literature. They identified four distinct types of methods: satellite-based methods, airplane-based methods, ground-based methods and field inventory. From these method types field inventory is by far the most common.

Satellite-based methods include very high resolution (VHR, i.e. sub-metre resolution) imagery and infrared scanning data acquired with instruments mounted on a satellite. Satellite-based methods can monitor large areas at once. However, the accuracy of the data is not sufficient for all applications of urban tree data. (Nielsen et al. 2014.) One example of a satellite-based urban tree inventory method is presented by Ardila et al. (2012). They identified the crowns of individual trees from VHR satellite images with object-based image analysis. The analysis consisted of several steps that aimed to identify trees of different sizes.

Airplane-based methods include data acquired with passive and active instruments mounted on an airplane. One of the active instruments used is the laser scanner. Like satellite-based methods, airplane-based methods can monitor large areas at once, although the simultaneously monitorable area is not quite as large, as the distance to the monitored area is significantly smaller. (Nielsen et al. 2014.) However, the smaller distance to the monitored area enables mapping the area with a somewhat better resolution. The article by Jutras et al. (2009) provides an example of an airplane-based urban tree inventory method. The method predicted urban tree attributes from ALS data with artificial neural networks.

Ground-based methods include photogrammetric methods and scanning methods. The scanning methods can be divided into terrestrial laser scanning (TLS) and mobile laser scanning (MLS). Ground-based methods provide detailed data on an individual tree level. However, the simultaneously monitorable area is very limited and thus ground-based methods are rather laborious. (Nielsen et al. 2014.) One ground-based urban tree inventory method is presented by Holopainen et al. (2013b). They detected and located trees from a multi-scan TLS point cloud by first finding the laser points most likely belonging to tree stems and constructing the trees using these stem points.

Field inventory methods include manual measurements and visual inspection of trees. Field inventory methods provide accurate data of different tree attributes. However, like other ground-based methods, they are rather time-consuming, as the area that can be monitored at once is very small. (Nielsen et al. 2014.) Thus, field inventory methods are often used for collecting reference data which can be used for assessing the accuracy of more efficient methods, such as satellite-based an airplane-based methods. Chacalo et al. (1994) provide an example of a typical field inventory method. They measured and estimated several tree attributes, such as tree height, species, diameter and health from numerous sample trees to gain an overall understanding of the condition of street trees in Mexico City.

4. Improving the vegetation point classification

Vegetation point extraction is the process of separating laser points originating from vegetation from other laser points in a laser point cloud. This process consists of two steps: laser point classification and improving the classification of vegetation points by separating real vegetation points from falsely classified vegetation points. The first of these steps includes separating ground returns from above-ground returns and assigning a class to each of the above-ground returns (e.g. building, low vegetation, high vegetation). In a rural environment, the classification step is sufficient, as there are no objects whose laser returns could mistakenly be interpreted as vegetation returns. In an urban environment, however, the situation is rather different, as the variety of objects is much larger (e.g. Liu et al. 2013).

Urban environments contain many man-made objects, such as buildings, cars, lamp posts and fences. Buildings are often easily detected, as they contain large, flat surfaces. In addition, the locations of buildings are often known beforehand and thus the laser returns corresponding with the building locations can be removed. However, the smaller man-made objects pose a problem, as they generate laser returns that have height values similar to trees and thus might be mistakenly interpreted as trees. In addition, these man-made objects can be located under trees, which further complicates their detection.

Most methods for separating man-made objects from vegetation have used spectral information provided by e.g. aerial imagery together with laser scanning data. One such method was presented by Zhang et al. (2015). They used hyperspectral images for determining whether a laser point originated from vegetation or some other object. This was done by calculating the NDVI (Normalised Difference Vegetation Index) for each cell of the hyperspectral data and using the value of each cell to classify the laser points falling within that cell.

Spectral information provides an efficient and effective way of separating vegetation laser points from other laser points. However, spectral data are not always available and in such cases the separating must be executed using only the laser scanning data. According to Liu et al. (2013), trees have two properties that can be used to distinguish them from man-made objects. Firstly, trees are irregular structures, as opposed to man-made objects that often consist of planar surfaces. Secondly, trees allow laser pulses to penetrate into deeper layers of the tree. This results in multiple returns from one laser pulse. Based on these two characteristics, Liu et al. presented a two-step method for separating vegetation laser points from laser points originating from other objects. First, the above-ground laser points are segmented using surface growing. Laser points that fit well on the same plane are grouped together. This results in segments of various sizes. Segments originating from vegetation contain smaller numbers of laser points compared to segments originating from man-made objects, as trees do not contain planar surfaces. Second, the segments created in the first step can be identified as vegetation or other based on the proportion of multiple returns. Segments originating from man-made objects contain mostly only first return laser points, whereas vegetation segments contain a larger number of second, third and even fourth return laser points. A similar method was presented by Höfle et al. (2012), but instead of surface growing, they used object-based raster analysis to create the preliminary segments.

5 Individual tree detection for measuring attributes of individual trees

The ALS-based methods for measuring tree and forest attributes can roughly be divided into two groups: Area-based methods (Naesset 1997, Næsset 2002) and individual tree methods (Hyyppä & Inkinen 1999). Area-based methods estimate forest attributes by creating a model between field measurements and the ALS data, whereas individual tree methods measure the attributes directly from the ALS data by detecting individual trees. Area-based methods have been more common until recent years, as individual tree-based methods require a high laser point density, which has been rather expensive to acquire (Vastaranta et al. 2012). However, recent development of laser scanners has lowered the costs of high point density ALS data resulting in it becoming more widely available (e.g. Lindberg & Holmgren 2017). In urban environments, individual tree methods have more potential, as urban trees often grow sparsely. Furthermore, the applications of tree and forest data in urban environments are rather different than those of non-urban forests and thus the data requirements differ significantly. Traditional forest inventory estimates forest variables that are related to the economic value of the forest (Holopainen et al. 2013a), whereas more precise attributes, such as the location and condition of individual trees are of interest in the case of urban trees (Tanhuanpää et al. 2014).

Individual tree methods measure forest variables on an individual tree level by identifying single trees from the ALS data. The tree attributes, such as tree height and crown diameter, can be measured directly from the ALS data, or they can be estimated by creating a model between field measurements and the ALS data (Yu et al. 2011). One major advantage of individual tree methods compared to area-based methods is the very limited need for field sampling (Holopainen et al. 2013a). In addition, individual tree-based methods can measure tree and forest parameters more accurately than area-based methods (Reitberger et al. 2009), as the parameters of each tree in the area of interest can be measured directly. The disadvantages of individual tree-based inventory methods include the need for high density ALS data and the computationally heavy processing of the ALS data (Vastaranta et al. 2012, Kaartinen et al. 2012).

The basic process of individual tree methods can be divided into three steps (Figure 10). First, the locations of individual trees are detected from the ALS data. This is most often done by finding local maxima of the data (Holopainen et al. 2013a). Next, the tree crowns are delineated. Several methods, such as watershed segmentation (e.g. Mongus & Žalik 2015) and region growing (e.g. Lu et al. 2014) are used for this task. Finally, different tree attributes, such as the tree height and crown diameter are determined from the delineated trees. Some attributes can be measured directly, and others must be estimated from the directly measured attributes (Holopainen et al. 2013a).

The first two steps of individual tree methods are called individual tree detection (ITD) (e.g. Holopainen et al. 2013a). ITD methods can roughly be divided into two classes: surface model methods and 3D methods (e.g. Lindberg & Holmgren 2017). Surface model methods use a canopy height model (CHM) constructed from the uppermost points of the ALS point cloud, ignoring the laser points reflected from deeper layers of the canopy. 3D methods, in contrast, take full advantage of the laser scanner's ability to acquire information also from the lower canopy layers by detecting trees using the whole point cloud.

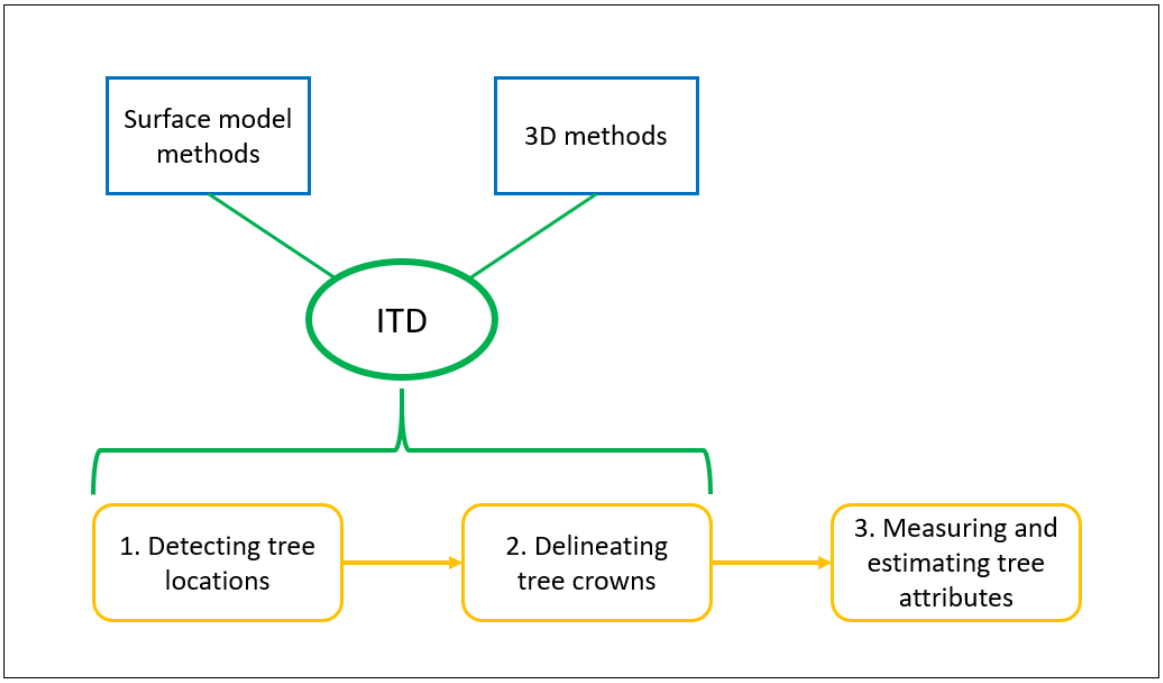

Figure 10 The process of individual tree-based forest inventory methods

The following two chapters will discuss surface model methods and 3D methods in more detail. Several implementations of both methods will be presented in addition to the basic theory of these methods. So far, the research on ALS-based ITD methods mostly covers non-urban forests. Thus, the majority of the methods presented in the following chapters are developed for and tested in non-urban environments. However, similar principles apply to ALS-based ITD in urban environments and most of the methods developed for non-urban environments can be used in urban environments with some modifications. The last chapter of this section will discuss the specifics of ITD of urban trees.

5.1 Surface model methods

Using a surface model has been the dominant method for ITD until recent years. The first articles discussing ITD using surface models were published around the end of the last century. Some of these articles include the publications of Hyyppä et al. (2001) and Persson et al. (2002). Hyyppä et al. (2001) detected tree crowns by creating a digital terrain height model (i.e. CHM) in raster format, filtering it with a simple low-pass filter to remove noise and identifying tree tops as the local maxima of the digital terrain height model. Then, they delineated the tree crowns from the digital terrain height model using the local maxima as seed points. Similarly, Persson et al. (2002) created a raster digital canopy model (i.e. CHM) and smoothed it with Gaussian filters of three different sizes to create three digital canopy models with different scales. Then, they detected tree tops as the local maxima in each digital canopy model. Finally, they fitted parabolic surfaces to the digital canopy model to determine which scale of the digital canopy model most accurately depicted reality in each area of the model.

These two methods describe the basic idea of surface model based ITD methods rather well. First, a CHM is created by subtracting the digital terrain model (DTM) representing the ground from the digital surface model (DSM) representing the topmost layer of the canopy (Figure 11). Thus, the CHM is a normalised DSM where the effect of changes in ground

height have been eliminated. Different surface model methods differ from each other in the way the DTM and DSM are created. As the DTM and DSM are most often in grid format, the height values in each grid cell must be defined in some way using the laser point cloud. The most common way of creating the CHM is the one used by Hyyppä et al. (2001) and Persson et al. (2002). They both created the DTM by determining the value of each grid cell from the minimum laser point height inside this cell. Similarly, the DSM was created by assigning the maximum laser point height value to each grid cell. If a cell included no laser points, its height value was interpolated using the values of neighbouring cells. Conversely, a more recent method created by Chen et al. (2006) used a canopy maxima model (CMM) as the surface model for tree top detection. Chen et al. (2006) first created a CHM in a similar way as Hyyppä et al. (2001) and Persson et al. (2002), but then created a CMM by assigning each grid cell the maximum height value of its neighbourhood. This way many false maximum points could be removed (Chen et al. 2006).

After creating a CHM, it is often smoothed to remove noise (Figure 11). In a way, the CMM created by Chen et al. (2006) can be seen as a smoothing method, as some variability in the data is removed when assigning the largest height value of the neighbourhood to each grid cell. Chen et al. (2006) used a Gaussian filter to further smoothen the CMM, as the neighbourhood used for creating the CMM was very small and thus not all false maxima could be removed. The filter size was chosen to be the same as the smallest estimated tree crown size in the area. Gaussian filters are also used in many other surface model methods, such as the ones presented by Persson et al. (2002), Yu et al. (2011) and Véga & Durrieu (2011). In contrast, Hyyppä et al. (2001) used a 3x3 weighted mean filter to smoothen the CHM. Regardless of the filtering method used, the size of the filter should be considered carefully to maximise its performance (Yu et al. 2011). The filter should be able to remove most of the noise in the CHM, but at the same time preserve all relevant information. If the kernel size is too small, not enough noise can be removed (Chen et al. 2006). Conversely, too large a kernel filters the image too much resulting in some trees not being detected.

The next step after smoothing is to detect tree tops as local maxima of the CHM (Figure 11). The basic idea is very simple – searching for the largest cell value in a defined neighbourhood. However, many methods apply additional constraints and preprocessing to minimise the possibility of detecting false tree tops. For example, Hyyppä et al. (2001) identified tree tops as the cells having the largest value in their 8-neighbourhood if their value was larger than a defined threshold. Tanhuanpää et al. (2014) applied a similar method in an urban environment, setting the threshold to 2.5 metres. This ensured that no low man-made objects, such as cars were falsely detected as trees. Yu et al. (2011) further processed the smoothed CHM by detecting regions with a minimum curvature method, used the region information to enhance the contrast of the CHM and detected local maxima from the contrast-enhanced CHM. Persson et al. (2002) had a rather different approach. They found the tree tops by placing starting points in every CHM cell having a value larger than 2 metres and always moving to the neighbouring cell with the largest value until a local maximum was found.

The final step of surface model-based ITD is to delineate the crowns of individual trees (Figure 11). The tree tops found in the previous step are often used as starting points for the delineation. Two of the most commonly used tree delineation methods are watershed segmentation and its inverse, the pouring algorithm (Tanhuanpää 2016). The method used by Persson et al. (2002) to detect tree tops is, in fact, watershed segmentation. Tanhuanpää (2016) described watershed segmentation as follows. Watershed segmentation first finds

local minima in the CHM. Then, it works its way to local maxima by always moving to the neighbouring cell with the largest height value. All cells that lead to the same local maximum are grouped to the same segment. Conversely, the pouring algorithm starts from local maxima and works its way to local minima in the opposite way as watershed segmentation. Articles discussing ITD often use the terms watershed segmentation and pouring algorithm interchangeably, as using the pouring algorithm is equivalent to using watershed segmentation on the inverse CHM. Many methods (e.g. Yu et al. 2011, Chen et al. 2006) use the tree tops as starting points and delineate tree crowns with watershed segmentation.

Some surface model-based ITD methods performed watershed segmentation on several scale levels and defined different metrics to select the appropriate scale level to be used in different parts of the CHM. One such example is the method by Straub (2003). Straub (2003) created a multi-scale representation of the CHM, segmented each scale level with a watershed algorithm and calculated several metrics, such as convexity and circularity to describe each segment. Then, they compared corresponding segments of each scale level based on the calculated metrics. The segments chosen to the final representation were the ones defined as most tree-like based on the metrics used. Other tree delineation methods of surface model-based ITD include region growing, and fitting surfaces and shapes to the CHM (Véga & Durrieu 2011). For example, Véga et al. (2011) created approximated tree crowns by fitting ellipsoids around the detected tree tops, whereas Hyyppä et al. (2001) used a region growing algorithm which delineated the tree crowns using height and distance-based thresholds.

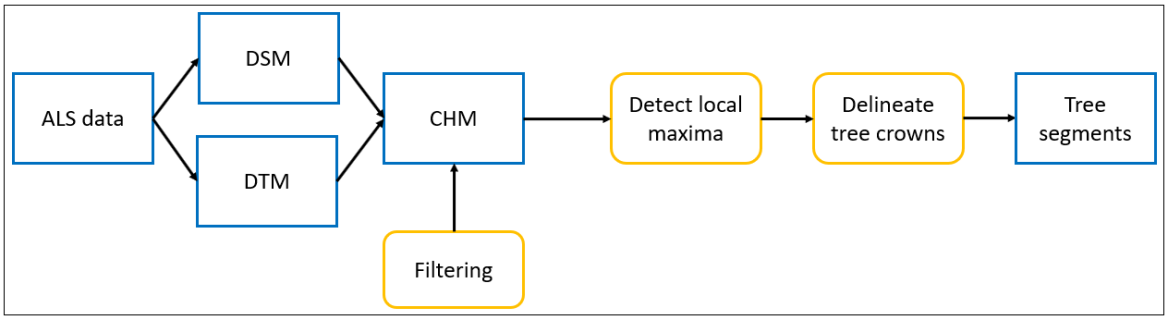

Figure 11 The process of surface model ITD methods. First, a CHM is created by subtracting the DTM from the DSM. Next, the CHM is filtered to remove noise. Then, tree tops are identified as local maxima in the CHM. Finally, tree crowns are delineated using the tree tops as starting points. The final result is a segmented CHM in which each segment represents one tree.

5.2 3D methods

The research on 3D-based ITD methods has gained popularity during recent years, as high-accuracy ALS data have become more widely available. 3D methods have great potential in ITD, but optimal methods have yet to be found (Lindberg & Holmgren 2017). There is a larger variety in the types of 3D methods compared to surface model methods. Thus, 3D methods cannot be described with a single process chart. However, the preprocessing steps of 3D methods are often rather similar. First, the ground points are separated from vegetation points. The ground points are then used for creating a digital terrain model (DTM). The final preprocessing step is normalising the vegetation points by subtracting the corresponding DTM height value from each vegetation point. See, for example, Li et al. (2012) for a more detailed explanation of the preprocessing.

Lindberg & Holmgren (2017) provided a review of 3D-based ITD methods. They grouped 3D methods into several categories based on the basic idea of the methods. Many 3D

methods do not lie just within one category but combine features from several categories. However, the grouping helps to understand the principles of 3D-based ITD methods.

One of the categories presented by Lindberg & Holmgren (2017) is a hybrid of surface model-based and 3D-based ITD. Methods belonging to this category first create a surface model of the point cloud. Then, they use the surface model to detect tree tops and possibly create an initial segmentation. The tree tops and initial segmentation are then used as input in segmenting the whole point cloud. One such method, created by Morsdorf et al. (2003), first created a digital surface model (DSM) grid from the point cloud and detected tree tops as local maxima in the DSM. Then, they clustered the point cloud with Euclidean distance-based k-means clustering using the local maxima as initial clusters. The vertical distance was scaled to take into account the somewhat elongated shape of trees. Duncanson et al. (2014) took another approach. They created a CHM from the point cloud and segmented it with watershed segmentation. Then, they created a histogram of laser point heights for each segment separately. Next, they inspected the histograms. If the histogram contained a clear trough (Figure 12), the laser points below the trough were separated from the histogram, as the trough suggested the presence of an understory tree. After each segment had been inspected, the point cloud was divided into two tree layers: an overstory and understory layer. The segmentation and division process was then repeated for the understory layer. The final result consisted of the segments of three tree layers.

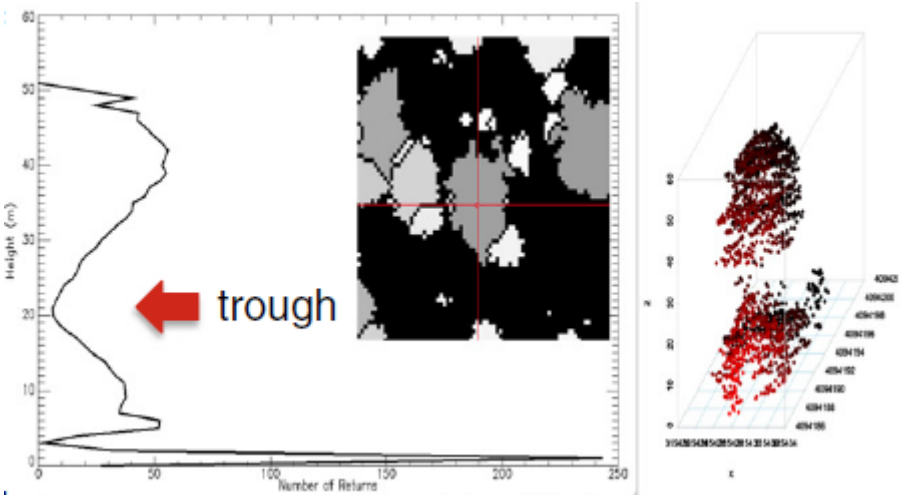

Figure 12 The histogram of one tree segment. There is a clear trough in the histogram, indicating an understory tree. The segment is shown with a red crosshair. The figure in the right presents the laser points belonging to the segment. (Duncanson et al. 2014)

Another 3D-based ITD category slices the point data horizontally to create slices of point cloud data, each belonging to a specific height range. Each slice is then segmented individually and finally, the corresponding segments of each slice are merged to create 3D tree segments. One slicing method is introduced by Tang et al. (2013). They first normalised the vegetation points by subtracting the DTM value from each point height. Then, they divided the normalised data to horizontal slices of equal vertical thickness. Next, they segmented the laser points of each slice with a regional level-set method. This resulted in contours describing the boundaries of individual trees. Finally, the tree boundaries of each slice were stacked to obtain the final 3D individual tree segments. Similarly, Kandare et al. (2014) normalised the laser points and divided them into slices with a 0.5-metre vertical interval. Only points with a height value over 1.5 metres were taken into account, as lower

points were considered as ground or ground vegetation reflections. They then clustered the points with k-means clustering for each horizontal slice separately. Next, ellipsoids were fitted around the centres of mass of the clusters in a top-down manner. If the centre of mass of a cluster lied within an ellipsoid created around a cluster with a higher centre of mass, the clusters were merged. After this, each cluster was inspected with a horizontal density function and split, if multiple density peaks were identified. Next, the clusters of different slices were merged by comparing horizontal polygons created around the clusters. The clusters of different slices were merged, if the overlap of their polygons was over 70 %. However, the clusters were again split, if multiple density peaks were identified in the vertical direction. The final segmentation was created by forming new horizontal polygons around the clusters and merging clusters with overlapping polygons, if the height distributions of the clusters were similar.

A third popular category in 3D-based ITD utilises region growing in the delineation of individual trees. Region growing methods can be divided into top-down and bottom-up methods. Top-down methods are far more common, as finding suitable starting points for region growing is much easier. Top-down methods start by identifying tree tops as highest points in their neighbourhood (see e.g. Lee et al. 2010). These local maxima are then used as seed points. One top-down region growing method was introduced by Li et al. (2012). They first normalised the vegetation points in the way described earlier. Next, they approximated the average crown radius and set this value as a threshold value. Then, laser points were examined one by one in a sequential manner starting from the highest point. The highest point was assumed to be a tree top of the first tree (tree A). The next highest laser point was either assigned to tree A or to a new tree based on a simple decision rule. If the horizontal distance between the laser point under inspection and the previously inspected laser point was smaller than the defined threshold, the laser point was assigned to tree A. Otherwise, the laser point was assigned to a new tree. Again, the next highest point was taken under inspection and the horizontal distances to the two previous points were calculated. The laser point was assigned to the tree with the shorter horizontal distance, or to a new tree, if neither of the horizontal distances were smaller than the threshold. This process was continued by always comparing the point under inspection to the lowest laser points of each tree until all vegetation points were segmented.

Bottom-up region growing methods start by identifying tree stems from the laser data. The stem points can be detected, for example, from the intensity information of the laser points (Lu et al. 2014) (Figure 13), or by classifying all vegetation points below a certain height level as stem points (Reitberger et al. 2009). The stems of individual trees can be delineated after the stem points have been detected. Reitberger et al. (2009) used RANSAC line fitting to delineate the stems (Figure 14), whereas Lu et al. (2014) started from the lowest stem points and used region growing based on horizontal and Euclidean distances to group points belonging to the same stem. Lu et al. (2014) continued the region growing process to delineate the crowns of individual trees. They assigned each non-stem vegetation point to a certain stem with rules based on 2D and 3D distances.

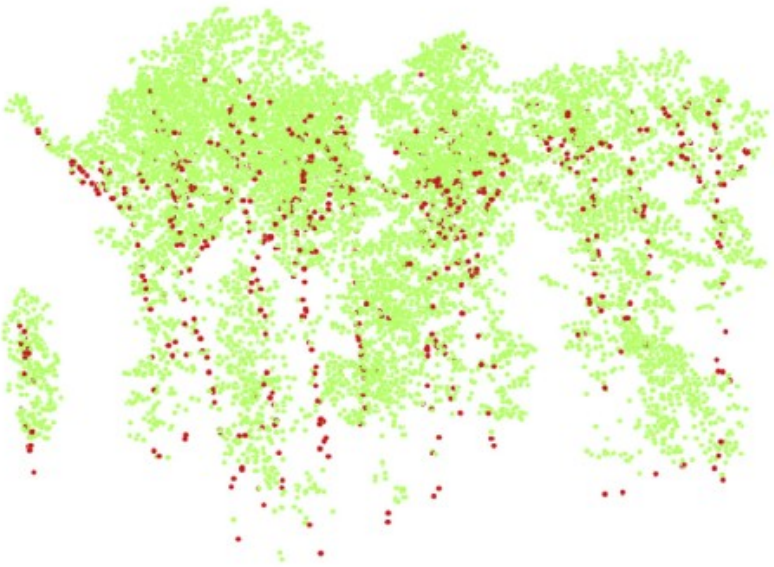

Figure 13 Classification of vegetation points based on intensity. The brown points represent stem points and green points represent non-stem points. (Lu et al. 2014)

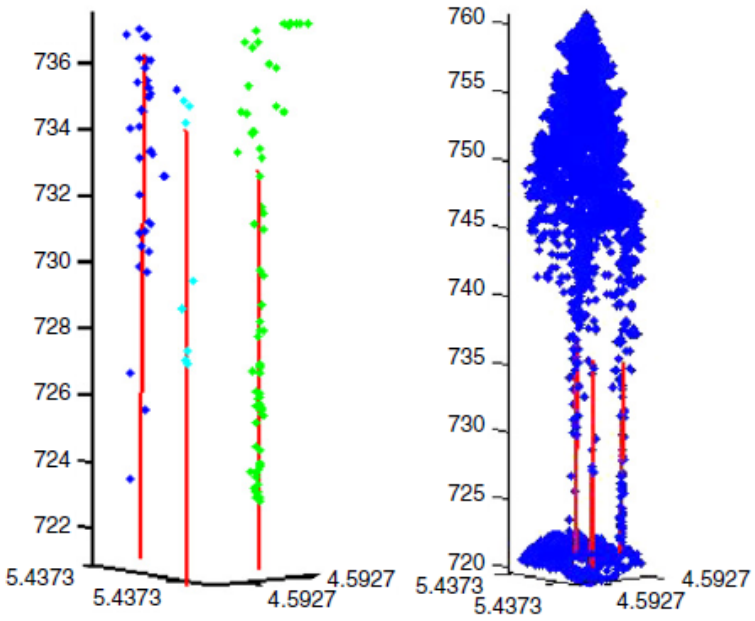

Figure 14 Stem points and RANSAC fitted lines representing the stems. (Reitberger et al. 2009)

Other 3D-based tree segmentation methods include the use of a mean-shift algorithm (e.g. Ferraz et al. 2012) or a normalised cut algorithm (e.g. Reitberger et al. 2009). In mean-shift segmentation, a kernel is used for grouping the laser points into segments. The kernel is centred to a laser point and it shifts from this point to the local point density maximum. All points from which the kernel shifts to the same density maximum are grouped to the same segment (Ferraz et al. 2012). Normalised cut segments the point data into groups using some criteria, such as the distance between points and the similarity of intensity values (Reitberger et al. 2009). The groups are formed in a way that maximises the similarity within groups and the dissimilarity between groups. (Reitberger et al. 2009).

5.3 Individual tree detection of urban trees

Individual tree detection in urban areas poses different kinds of challenges compared to non-urban forests. Urban trees are located close to man-made structures, such as buildings, lamp posts and vehicles, which can complicate the detection of trees (Zhang et al. 2015). For this reason, the vegetation points should first be extracted before mapping and measuring the attributes of individual trees. Another challenge with urban tree detection is the diversity of urban forests (Zhang et al. 2015). Rural forests often consist of trees of the same species and thus the shape and size of the trees is somewhat similar. This allows creating ITD methods that suit a specific type of forest. Urban forests, in turn, consist of trees of various species, sizes and shapes and thus finding a suitable method for detecting and delineating individual trees can be rather challenging.

Most ITD methods of urban trees developed so far have used remote sensing imagery (e.g. Ardila et al. 2012). However, imagery limits the analysis to two dimensions. To overcome this problem, more recent research has explored the possibility of using laser scanning to detect and delineate urban trees. Most of the research has combined laser scanning data with aerial images (e.g. Yao & Wei 2013, Zhang et al. 2015). Methods purely based on ALS data are very rare.

One recent urban ITD method combining aerial images and laser scanning data was introduced by Zhang et al. (2015). They first separated the ground laser points from above ground laser points and created a DTM. Then, they identified the vegetation laser points from the above ground points with the help of a normalised difference vegetation index (NDVI) image created from hyperspectral data. The laser points were compared to their spatially corresponding cell of the NDVI image. If the NDVI value of the corresponding cell was larger than zero, the laser point was identified as a vegetation point. Next, the tree tops were identified from the vegetation points using a tree climbing algorithm. The algorithm first detects the tree tops as local maxima in the data and then removes local maxima that are located within a horizontal threshold distance to a higher local maximum. The final step of the method was delineating the tree crowns using the tree tops as centre points. The boundary of a tree was found by comparing the average heights of laser points falling within different horizontal distances from a tree top. The tree boundary was placed to the horizontal distance with a minimum average height and all vegetation points falling within this horizontal distance were segmented to the same tree.

One of the rare urban ITD methods using only ALS data was introduced by Liu et al. (2013). Liu et al. first separated the ground laser points from the non-ground laser points using a slope-based filter and created a DTM from the ground points. Then, they separated the vegetation laser points from other above ground laser points (e.g. buildings and vehicles). The separation was based on the two distinct properties of vegetation points: They do not fit well on the same plane and they consist of multiple echoes. The first step of separating vegetation points included the use of a surface growing algorithm. The surface growing algorithm creates planes from adjacent laser points. These planes are called seed surfaces. Then, additional laser points are added to the planes if they are located close to a seed surface or fit well on a seed surface. The result consists of surfaces of different sizes. Large surfaces correspond to buildings whereas trees consist of many small surfaces. Thus, the laser points belonging to smaller surfaces are identified as vegetation points. The second step of separating vegetation points was multiple return analysis. The points in each surface segment found in the previous step were inspected. If the segment contained a large proportion of

multiple return points, the points in the segment were classified as vegetation points, as vegetation often creates multiple returns (Figure 15). The tree crowns were delineated after extracting the vegetation points in the two previous steps. First, the vegetation points were clustered. Then, the tree tops were identified as local maxima in the clusters. False tree tops were removed by defining a horizontal threshold distance and removing tree tops that were located within this threshold distance from a higher tree top. The threshold distance was based on the average height of the cluster points. A larger average height resulted in a larger threshold distance, as the tree height and crown size are directly proportional. Next, the boundaries of individual trees were delineated using a spoke wheel (Figure 16). A raster was created from the laser data by placing the raster on top of the laser points and selecting the elevation of the highest laser point as the value of each raster cell. Then, the spoke wheel was centred on each raster cell representing a tree top. After this, the intersections between the tree boundary and each spoke of the spoke wheel were found by comparing the height differences of each spoke cell and the tree top. After these intersections were found, the tree boundary polygon was formed by connecting each intersection point (Figure 17).

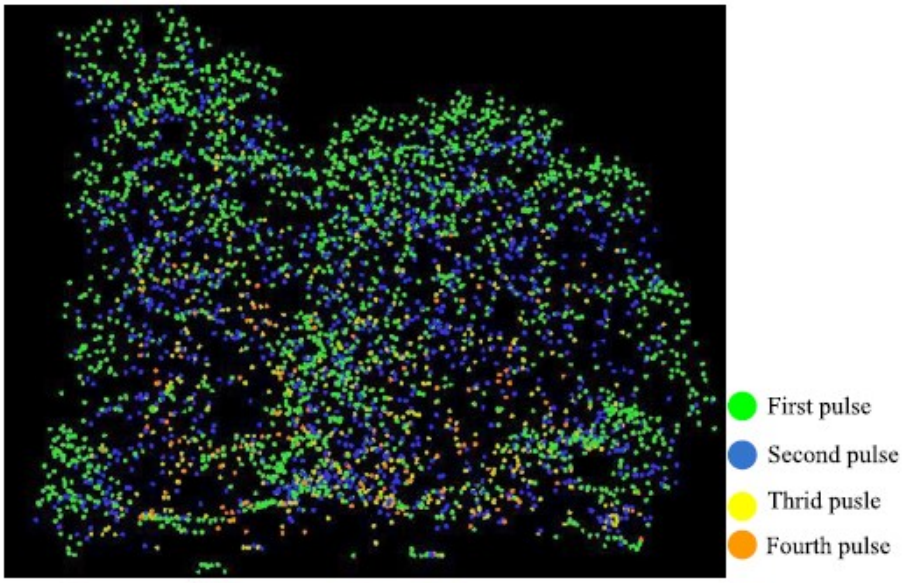

Figure 15 The laser returns of a tree (Liu et al. 2013)

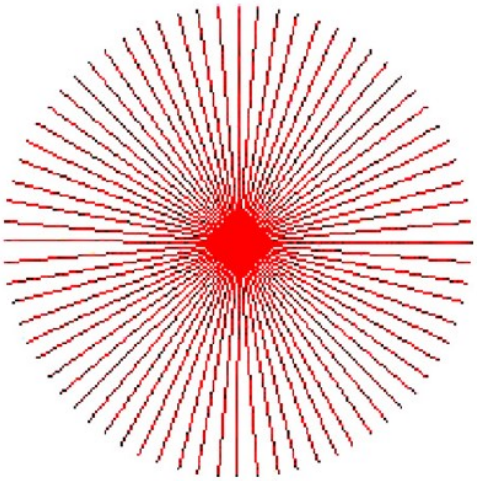

Figure 16 A spoke wheel (Liu et al. 2013)

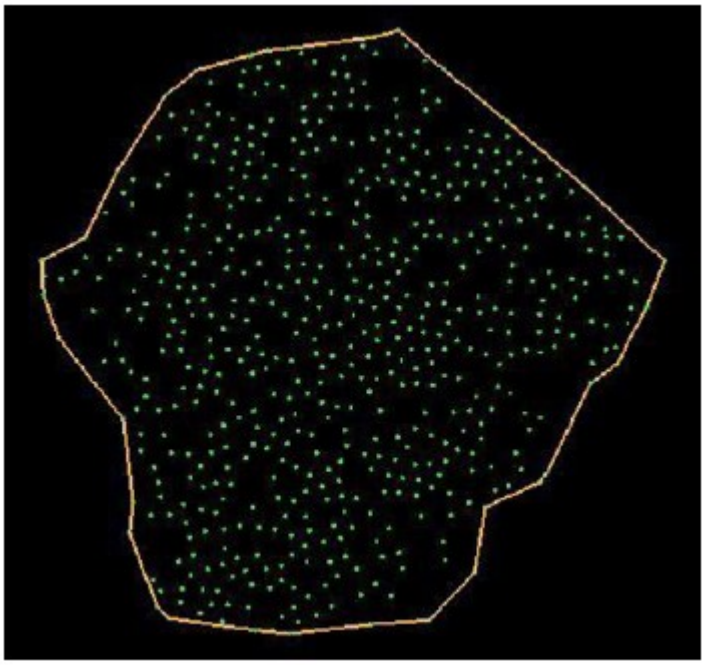

Figure 17 The tree boundary (Liu et al. 2013)

6 Material and methods

6.1 Data

The laser data used in this study (Figure 18) were acquired with the Optech Titan multispectral laser scanner in the summer of 2017. The specifications of Optech Titan are presented in Figure 19. The point density of the data was approximately 50 points/m^2. The data were pre-classified by the city of Helsinki according to the ASPRS (American Society for Photogrammetry and Remote Sensing) LAS standard. The resulting classes are presented in Table 1. An RGB colour code was added to each point of the laser point cloud based on aerial images acquired in 2017.

Figure 18 A side view of the laser data. Each laser point has been given an RGB value from aerial images.

Parameter	Specification
Laser Configuration	
Channel 1	1550 nm IR
Channel 2	1064 nm NIR
Channel 3	532 nm visible
Beam divergence	Channel 1 & 2: ≈0.35 mrad (1/e) Channel 3: ≈0.7 mrad (1/e)
Laser classification	Class IV (US FDA 21 CFR 1040.10 and 1040.11; IEC/EN 60825-1)
Operating altitudes [1,2]	Topographic: 300 - 2000 m AGL, all channels Bathymetric: 300 - 600 m AGL, 532 nm
Depth performance [1,4]	Dmax (m) ≈ 1.5/K_d, where K_d is the diffuse attenuation coefficient of the water
Effective PRF	Programmable; 50 - 300 kHz (per channel); 900 kHz total
Point density [4]	Bathymetric: >15 pts/m2 Topographic: >45 pts/m2
Scan angle (FOV)	Programmable; 0 - 60° maximum
Effective scan frequency	Programmable; 0 - 210 Hz
Swath width	0 - 115% of AGL
Horizontal accuracy [2,3]	1/7,500 × altitude; 1 σ
Elevation accuracy [2,3]	< 5 - 10 cm; 1σ
Laser range precision [5]	< 0.008 m; 1 σ
Camera Configuration	
Q/A camera	29 MP RGB/CIR; 5.5 µm pixel; 6,600 x 4,400 pixels; 0.5 sec/frame
Medium format camera (optional)	80 MP RGB/CIR; 5.2 µm pixel; 10,320 x 7,760 pixels ; 2.5 sec/frame

Figure 19 Specifications of Optech Titan (Teledyne Optech 2015)

Table 1 The pre-classification classes

Class number	Definition
0	Created, never classified
1	Unclassified
2	Ground
3	Low Vegetation
4	Medium Vegetation
5	High Vegetation
6	Building
7	Low Point (noise)
8	Keypoint
9	Water
10	Rail
11	Road Surface
12	Isolated Points
13	Wire - Guard (Shield)
14	Wire – Conductor (Phase)
15	Transmission Tower
16	Wire-structure Conductor
17	Bridge Deck
64	High Noise
65	First Pulse
66	Overlap
67	Building Roofs
68	Edge Building
69	Ground Inside Building
70	Wall
71	Wall Structure
72	Roof Structure
73	Air
74	Vegetation
75	Tree
76	Tall Tree
77	Tree Tip
78	Pole
79	Car

6.2 Study Area

The study area consisted of 70 small sample plots located in the city of Helsinki (Figure 20). The sample plots consisted mainly of street trees, but also some park trees were included. The plots contained 3239 field measured trees that belonged to 15 genera. The most common genera were Tilia (lime), Betula (birch) and Acer (maple) (Table 2).

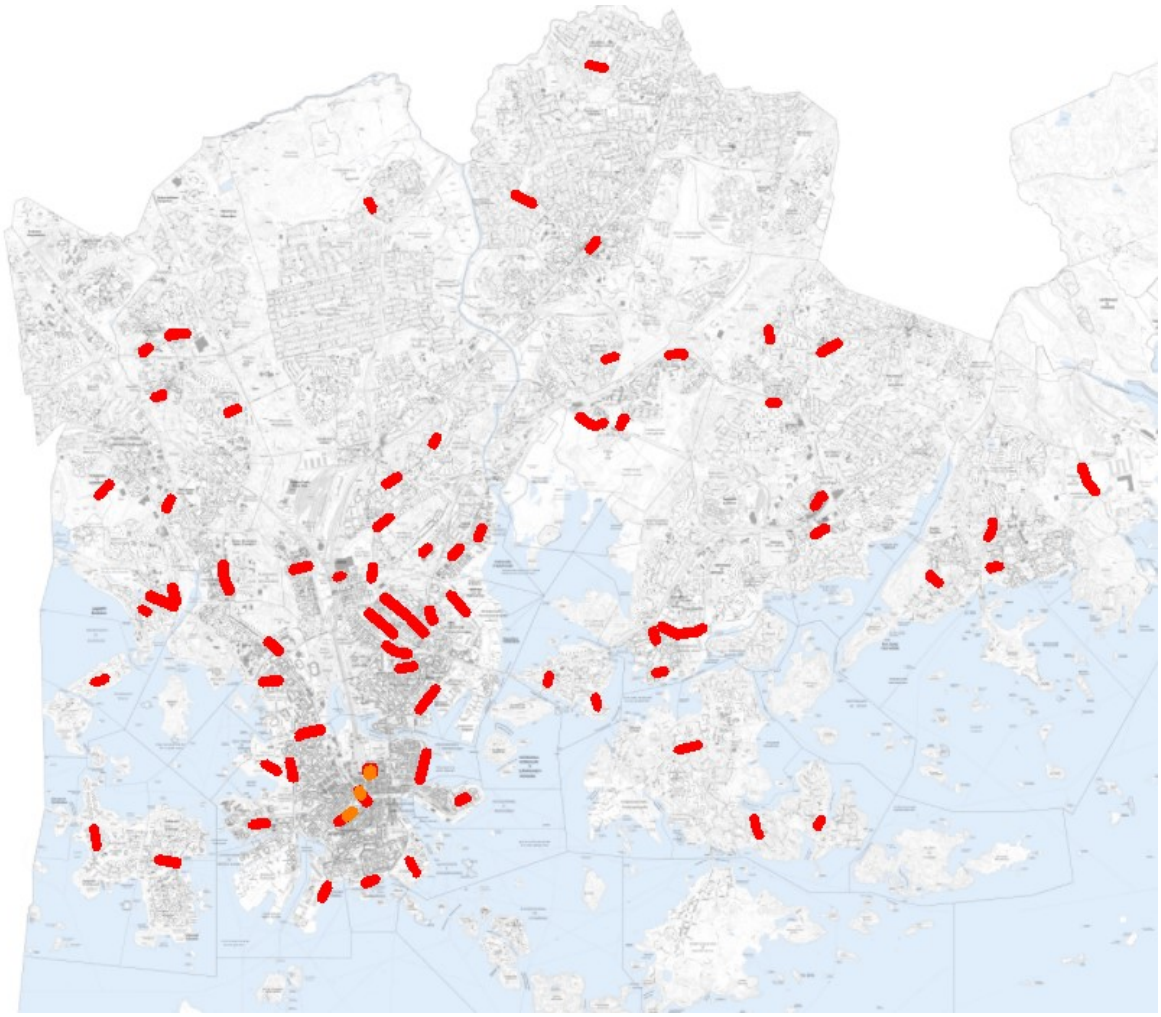

Figure 20 The locations of the sample plots. The sample plots used for inspecting the performance of the cleaning algorithm are presented in orange. The sample plots used for assessing the performance of the ITD methods are presented in red.

Table 2 Tree genera and their occurrences in the sample plots

Genus	**Number of trees**
Tilia	1904
Betula	327
Acer	259
Ulmus	221
Quercus	160
Aesculus	65
Populus	65
Sorbus	60
Prunus	53
Malus	51
Pinus	32
Crataegus	21
Salix	19
Alnus	1
Amelanchier	1

6.3 Pre-processing of the data

The ALS data were pre-classified by the city of Helsinki. The classes of the pre-classification are presented in Table 1. The classification was performed with a simple process based on the height from ground. First, a DTM was created from ALS points identified as ground points. Next, all other points were classified using their height from the DTM. Points with heights of 0-0.2, 0.2-2 and 2-500 metres were classified as low, medium and high vegetation respectively. Finally, points belonging to large planes were identified as rooftops and removed from the vegetation classes.

The pre-classified point cloud was further processed with Terrascan software to extract the vegetation points from the point cloud. Not all buildings had been identified and thus the vegetation classes contained points that in reality belonged to buildings. These points were removed using building masks. After this, the point heights were normalised by subtracting the DTM height from the height of each point. Finally, points with a height under one metre were removed from the point cloud and only the points belonging to the medium and high vegetation classes were exported for further processing.

6.4 Improving the vegetation point classification

The vegetation points of the pre-processed data contained falsely classified points, as some man-made objects were mistakenly interpreted as vegetation. A cleaning algorithm was created and tested for removing these false vegetation points. Matlab software was used for creating the algorithm and assessing its performance. The cleaning algorithm was created from scratch, although some of Matlab's readily available functions and libraries were utilised. The algorithm was based on the method presented by Liu et al. (2013). The method presented by Liu et al. exploits the two characteristics that allow identifying and separating trees from other objects: Trees do not consist of large planar surfaces and laser pulses hitting trees create multiple echoes. Thus, the method is divided into two parts: Segmenting the point cloud into planar surfaces (surface growing) and calculating the proportion of multiple echoes in each surface segment. The surface growing algorithm used was based on Rabbani et al. (2006). The algorithm works as follows:

Surface growing

1. Estimate the normal vector of each laser point by fitting a plane to the neighbourhood of the point and setting the plane normal as the normal vector of the point. The 10 nearest neighbours were used as the neighbourhood of each point.
2. Similarly, calculate the residual of each point by fitting a plane to the neighbourhood of the point and calculating the point residual of the plane-fit. The 10 nearest neighbours were used as the neighbourhood of each point.
3. Sort the laser points into ascending order based on their residual. Define a residual threshold RTH as the 95^{th} percentile of the point residuals.
4. Define an angle threshold ATH. The angle threshold determines the maximum angle allowed between the normal vectors of two points for the points to be segmented to the same planar surface. Angle thresholds of 5, 7 and 9 degrees were used in this study.
5. Select the first point from the point list PL which contains the laser points sorted into ascending order based on their residual. This point is the first seed point SP of a new segment S.

6. Inspect the 10 nearest neighbours of SP. All neighbouring points whose normal vector between the normal vector of SP is smaller than the angle threshold ATH are assigned to segment S. Remove these points from the point list PL. Of these points, the points with a residual smaller than RTH are assigned as new seed points of S.
7. Repeat step 6 with each new seed point SP until segment S contains no more seed points (Note that new seed points may again be found when going through step 6 with each seed point).
8. Go back to step 5 and repeat steps 5-7 until the point list PL contains only points with a residual larger than the threshold RTH. The result is a point cloud segmented into almost planar surfaces.

Multiple return analysis

9. Inspect the points in each segment. If the segment contains less than 11 points, store the points in the segment as vegetation points. Otherwise, calculate the proportion of multiple returns (second, third, fourth and fifth returns) of all returns in the segment. If the proportion is larger than 25 %, store the points in the segment as vegetation points and remove the points otherwise.

6.5 Individual tree detection

Three ITD algorithms were tested in this study. The first, second and third algorithm were based on the methods presented by Lu et al. (2014), Kandare et al. (2014) and Duncanson et al. (2014) respectively. All these methods were originally developed for rural forests. These three methods were selected, as they all represented a different 3D-based ITD category (see chapter 5.2) and thus the methods differed from each other quite a bit. The algorithms were created from scratch with Matlab software and following the guidelines of the articles by Lu et al. (2014), Kandare et al. (2014) and Duncanson et al. (2014). Matlab's readily available libraries and functions were utilised when creating the algorithms. The following chapters present these algorithms in more detail.

6.5.1 Method 1: A bottom-up approach to segment individual deciduous trees using leaf-off lidar point cloud data

The method created by Lu et al. (2014) falls in the region growing category. The method was originally tested with leafless trees, as the test dataset was acquired in the winter. The method starts by dividing the vegetation points into stem points and non-stem points based on their intensity. Next, the tree stems are delineated from the stem points with a bottom-up growing algorithm. The algorithm goes through the stem points starting from the bottom-most one and assigns points to different stems based on their horizontal distance. After a certain height threshold (15 m in the article) also the 3D distance is considered, as trees can overlap each other in the higher parts of the canopy. Once the stems have been delineated, the non-stem points are assigned to the stems based on horizontal and 3D distance criteria. Figure 21 presents the process chart of the method. The detailed algorithm is described as follows:

Division of vegetation points

1. Divide the vegetation points into stem points and non-stem points based on an intensity threshold. The intensity threshold used was 35, which was the same as the threshold used by Lu et al. (2014).

Stem delineation

2. Arrange the stem points in ascending order based on elevation.
3. Select the first (bottom-most) point SP1 and assign it to tree T1.
4. Select the next point SP2. If the horizontal distance between SP1 and SP2 is smaller than a defined threshold HTH, assign point SP2 to tree T1. Otherwise assign SP2 to a new tree T2. The horizontal threshold was defined as

$$HTH = \frac{median(hpdist(VP))}{10}, \quad (5)$$

   where VP are the vegetation points and hpdist is a function that calculates the horizontal distances between every tenth vegetation point in the point cloud. The denominator of equation (5) was selected based on trial and error.
5. Select the next point SP3. If the horizontal distance between SP3 and at least one tree is under the HTH, assign SP3 to the closest tree (the tree with the closest point). Otherwise, assign SP3 to a new tree C.
6. Continue, until the point heights are over an elevation threshold ETH. Once ETH is reached, a 3D distance criterion is added. The elevation threshold was defined as the 85^{th} percentile of the heights of the vegetation points.
7. Select the next point SPn (whose height is over ETH). Find the tree that has the smallest 3D distance to SPn. If the horizontal distance between SPn and the tree is under HTH, assign SPn to the tree. Otherwise, assign SPn to a new tree Tm.
8. Continue, until all stem points have been processed
9. Inspect the delineated stems. Delete the stems whose length (height difference between highest and lowest point) is under a defined threshold.

Tree-trunk-growing

10. Arrange the non-stem points in ascending order base on elevation.
11. Select the first (bottom-most) point NP1. Find the tree that has the smallest 3D distance to NP1. If the horizontal distance between NP1 and the tree is under HTH, assign NP1 to the tree. Otherwise, store the point for further processing.
12. Continue step 11 for all non-stem points.

Final allocation

13. Go through the non-stem points that were not classified in tree-trunk-growing.
14. For each point, find the tree that has the smallest 3D distance and assign the point to that tree.

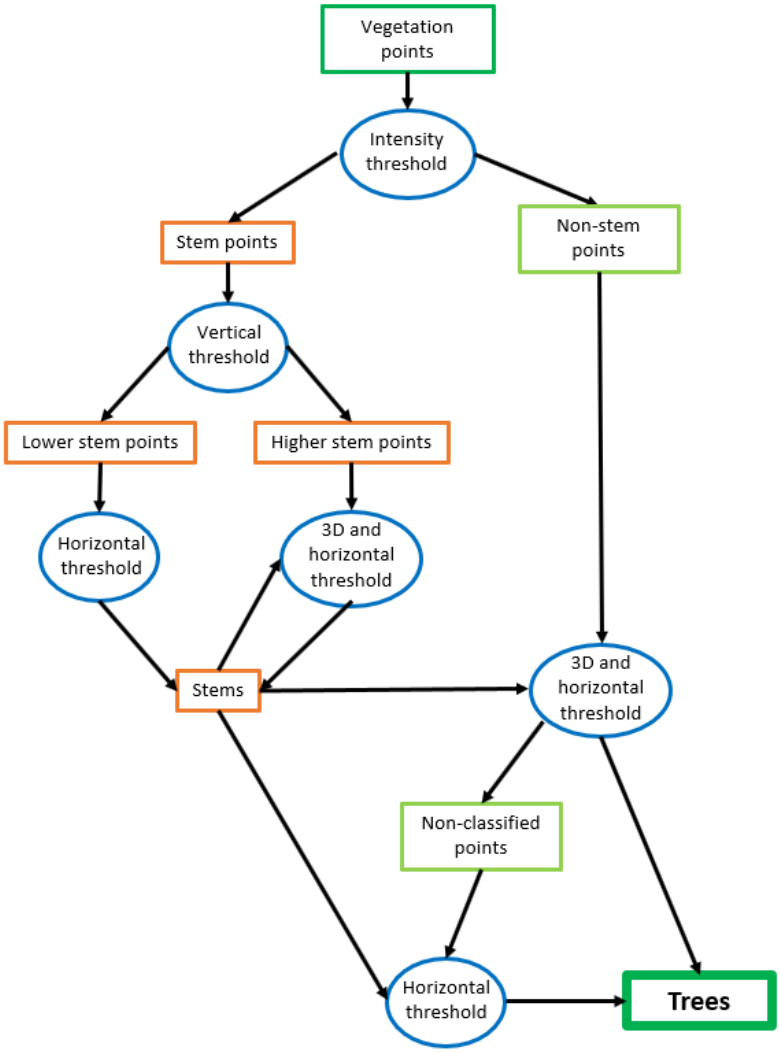

Figure 21 The process chart of ITD method 1

6.5.2 Method 2: A new procedure for identifying single trees in understory layer using discrete lidar data

The method presented by Kandare et al. (2014) delineates trees by first grouping point cloud data belonging to a specific height range and then merging the groups of different height ranges. The point cloud data is first divided into horizontal slices with a specific vertical thickness. Then, the points in each slice are clustered using k-means clustering. Next, some of the formed clusters are merged based on additional criteria. Finally, the overlapping clusters of consecutive slices are merged. Figure 22 presents the process chart of the method. The detailed algorithm is described as follows:

Horizontal slicing

1. Divide the point cloud data into horizontal slices of a certain vertical thickness starting from a threshold height. The points under the threshold height are ignored. The vertical thickness and starting height used in this study were 1 metre and 1.5 metres.

Clustering the slices

2. Cluster the points in each slice with K-means clustering. The optimal number of clusters is defined with the elbow method. The elbow method clusters the data with several values of k and selects the value of k that explains a chosen percentage of the variance in the data (e.g. Bholowalia & Kumar 2014). A 99.9 % variance threshold was used in this study.
3. For each slice:
    a. Calculate the mean coordinates (barycentre) of each cluster and sort the clusters in descending order based on the mean z-coordinate.
    b. Select the highest cluster C1 (the cluster with the largest mean z-coordinate).
    c. Fit an ellipsoid around C1. The axes of the ellipsoid are equal to the x, y and z coordinate ranges of the cluster. The ellipsoid is centred at the cluster barycentre.
    d. Inspect the barycentres of the other clusters. If the barycentre of a cluster is located within the ellipsoid, merge this cluster with cluster C1.
    e. Repeat steps b-d, until all clusters in the slice have been handled.

Merging the clusters of consecutive slices

4. Select the lowest slice S1 and the second lowest slice S2
5. For each cluster Ci in S1:
    a. Create a horizontal convex hull polygon Pi around Ci.
    b. Calculate the overlap percentages of Pi and the horizontal convex hull polygons created around each cluster in S2. Merge all clusters with Ci that have an overlap percentage larger than a defined threshold (60 % was used in this study).
6. Repeat steps 4 and 5 for each slice.

Removing small clusters

7. Remove the clusters that contain less points than a defined threshold. 40 points was found to be a suitable threshold after experimenting with several different values.

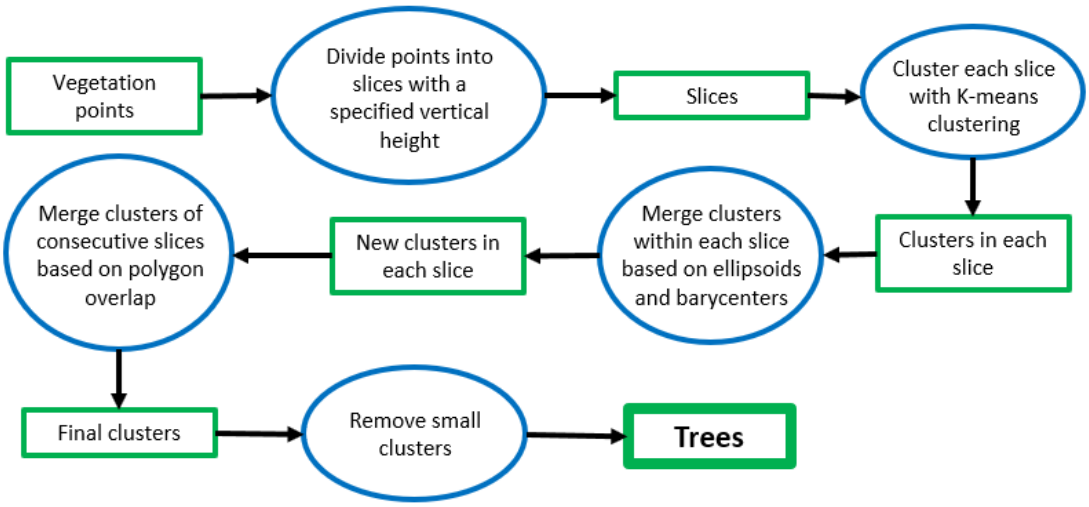

Figure 22 The process chart of ITD method 2

6.5.3 Method 3: An efficient, multi-layered crown delineation algorithm for mapping individual tree structure across multiple ecosystems

The method presented by Duncanson et al. (2014) is a hybrid of surface model and 3D ITD methods. The method creates a canopy height model (CHM) of the point cloud and segments it with watershed segmentation. Then, it inspects the height histograms of each segment. If the height histogram contains a clear trough (see Figure 12), the segment is divided into two segments – one that contains the points that have a height value larger than the trough height and one that contains the rest of the points in the segment. When all segments have been inspected, the points of the divided segments are assigned to an overstory and understory layer and the process is repeated starting from the CHM creation for both layers. This process enables the detection of understory trees that are located under higher trees. Figure 23 presents the process chart of the method. The detailed algorithm is described as follows:

CHM creation

1. Create a raster CHM of the point cloud data. A raster cell size of 0.5 metres was used in this study. Each CHM cell is assigned the height value of the highest point falling within the cell.
2. Define a threshold height. All CHM cells with a value smaller than the threshold are classified as ground cells and set to zero. A height threshold of 2 metres was used in this study.
3. Smooth the CHM with a moving window average filter. A window size of 5x5 cells was used in this study.

Marker-controlled watershed segmentation

4. Highlight the foreground and background markers of the CHM using morphological operators (see MathWorks 2018).
5. Segment the foreground and background highlighted CHM with watershed segmentation.

Trough search

6. For each segment:
    a. Create a histogram of the segment point heights.
    b. Search for troughs in the histogram. If a trough is found, split the segment into two segments – one that contains the points above the trough (overstory points) and one that contains the points below the trough (understory points)
7. Divide the point cloud data into an overstory and understory layer. Assign the overstory points of each segment into the overstory layer and the understory points of each segment into the understory layer. The points of the segments that were not split are assigned to the overstory layer.
8. Repeat steps 1-7 for the overstory and understory layers separately.

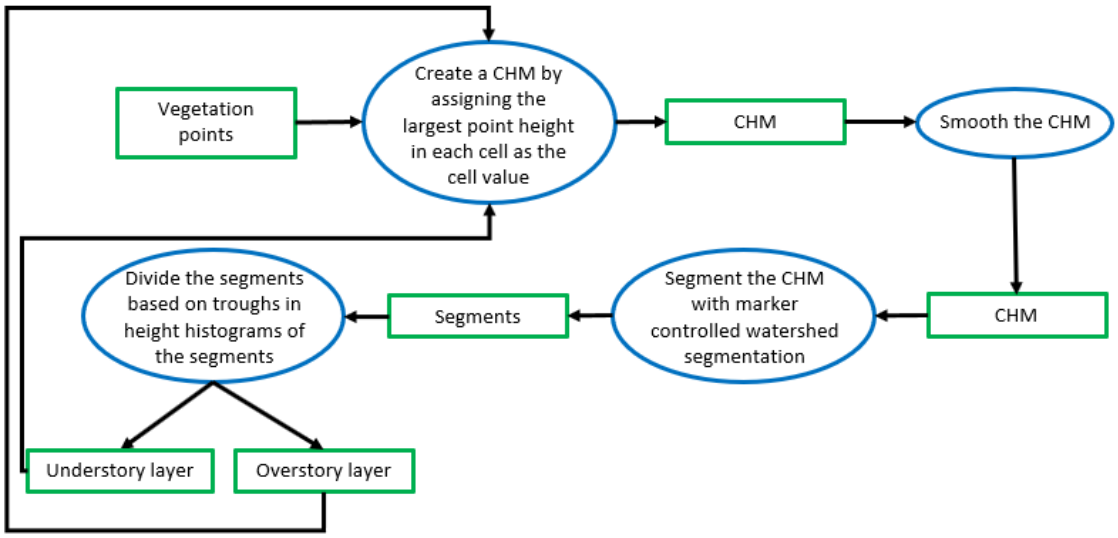

Figure 23 The process chart of ITD method 3

6.6 Accuracy assessment

6.6.1 Improving the vegetation point classification

The performance of the algorithm created for detecting and removing falsely classified vegetation points (i.e. the cleaning algorithm) was tested by visually assessing the results of the algorithm on three sample plots (Figure 20). The visual assessment consisted of inspecting how well various man-made objects were detected and removed from the vegetation points. The algorithm was tested with three different angle thresholds: 5, 7 and 9 degrees. Orthophotos and Google Street View images were used in the assessment to help identify the various objects. The man-made objects were grouped into five classes (Table 3). A rooftop class was included in the inspection even though most buildings were already removed from the data (see chapter 6.3), as the data contained temporary buildings and structures that could not be removed with the building masks.

Table 3 The classes of man-made objects that were inspected.

Class	Examples
Bus/tram stops	Sheltered bus and tram stops
Cables	Tram wires and other overhead lines
Vehicles	Cars, trucks, buses and trams
Vertical poles	Lamp posts, traffic signs and flag poles
Rooftops	Rooftops of temporary buildings and structures

6.6.2 Individual tree detection

The performance of the three ITD methods was assessed by comparing the delineated trees to reference data. The reference data contained information about field measured trees collected between years 1995 and 2017. The attributes of the reference data included the tree genus, species, DBH, location and height in addition to a few attributes not relevant to this

study. However, not all attributes were recorded for all trees in the reference data. The reference data were checked by projecting the location of each tree on top of aerial orthophotos acquired in 2017. Some trees had a slightly incorrect location and some trees no longer existed in the orthophotos. These trees were moved to the correct location or removed from the reference data. After correction, the reference data contained 3239 reference trees. The distribution of the reference tree genera is presented in Table 2.

The location and height were calculated for each delineated tree. The location was defined as the median of the easting and northing of the laser points belonging to a tree. The reason for using median instead of mean was that the delineated trees often contained some isolated points that distorted the location of the tree. The tree height was defined as the 99th percentile of the heights of the points in a tree. The 99th percentile was used instead of the maximum height, as again the delineated trees contained some noise points that did not represent the true dimensions of the tree.

The delineated trees and reference trees were matched using a distance threshold. The distance threshold defined whether a matching delineated tree was found for a reference tree and vice versa. If one or more delineated trees were located within the threshold distance of a reference tree, the closest delineated tree was matched with the reference tree. Otherwise, the reference tree was defined as a non-detected tree. Once a delineated tree was matched with a reference tree, it was removed from the data to prevent matching it with another reference tree. The tree matching process was performed with distance thresholds ranging from 0.5 metres to 6 metres with an interval of 0.5 metres. Several distance thresholds were tested, as the exact location of the tree stem is very hard to estimate from the laser point cloud and thus the detection rate of trees depends on the maximum allowed locational difference between the delineated trees and real (reference) trees. A small distance threshold results in less trees being detected, whereas a very large distance threshold results in all trees being detected.

The matches between delineated trees and reference trees were recorded in confusion matrices. In total, 36 confusion matrices were created – one for each ITD method and distance threshold. The reference trees were classified into different types based on their genus and height. Each column in the confusion matrices represented one reference tree type (e.g. Tilia 10-15 m). Some reference trees did not have height information and thus an additional no height column was created for each genus. The delineated trees, in turn, were classified into different height ranges and each row in the confusion matrices represented one height range of delineated trees (e.g. tree 10-15 m). In addition to the different tree types, the confusion matrices contained a no tree row and column to store the instances where no correspondence was found for a delineated tree in the reference trees or vice versa. An example confusion matrix is presented in Appendix 1.

The values for each cell in the confusion matrices were calculated in the following way:

1. Pick one reference tree and store its genus and height.
2. Search for the closest delineated tree whose location is within a defined threshold distance from the location of the reference tree.
    a. If such tree is found, increment the cell that corresponds with the genus and height of the reference tree and the height of the delineated tree. Remove the matched delineated tree from the data, so that it will not be matched with any other reference tree.

   b. If no such tree is found, increment the cell on the no tree row that corresponds with the genus and height of the reference tree.
3. Repeat steps 1 and 2 until all reference trees have been checked
4. For all delineated trees that did not correspond with any reference tree, increment the cell on the no tree column that corresponds with the height of the delineated tree.

The main accuracy measures used for assessing the performance of the ITD methods were precision – the fraction of real trees of all delineated trees – and recall – the fraction of real trees identified. Precision measures how prone the methods are to erroneous tree detection and recall describes how well the methods detect the trees. The equations for precision and recall are the following:

$$Precision = \frac{TP}{TP + FP} \tag{6}$$

$$Recall = \frac{TP}{TP + FN}. \tag{7}$$

In equations 6 and 7 TP, FP and FN denote true positives, false positives and false negatives, respectively. True positives are the correctly identified trees, false positives the falsely identified trees and false negatives the trees that were not identified.

The measures calculated for each ITD method were overall precision, overall recall, recall per reference tree genus and recall per reference tree height. The overall measures and height specific measures were calculated using observations of all genera. However, the genus specific measures were calculated only for the three most frequent genera – Tilia, Betula and Acer. In all measures, the number of true positives was defined as the number of reference trees for which a corresponding delineated tree was found regardless of whether these trees fell within the same height range. When calculating the overall precision and recall, all information of the genera and heights were discarded, and the true positives were calculated simply as the occurrences where a corresponding delineated tree was found for a reference tree. The precision measure could not be calculated for the reference tree genera separately, as the delineated trees did not contain genus information and thus the false positives could not be directed to a certain genus.

7 Results

7.1 Improving the vegetation point classification

The detection accuracies of the various man-made objects were described using four classes (Table 4). The accuracy was estimated visually for each object class separately. The resulting detection accuracies are presented in Table 5. Table 5 shows that the detection accuracies increased with larger angle thresholds used in the cleaning algorithm. Bus and tram stops were detected most accurately followed by vehicles and rooftops of temporary structures. The detection of cables and vertical structures was very poor.

Table 4 The classes used for estimating the detection accuracy of the cleaning algorithm

Class	**Description**
Not detected	None or very few of the points belonging to the object class were detected.
Poorly detected	Approximately 25 % of the points belonging to the object class were detected.
Partially detected	Approximately 50 % of the points belonging to the object class were detected.
Well detected	Approximately 75 % of the points belonging to the object class were detected.
Fully detected	Over 90 % of the points belonging to the object class were detected.

Table 5 The detection accuracies of each object class

		Angle threshold		
Object class	**Number of objects in sample plots**	**5°**	**7°**	**9°**
Bus/tram stops	7	Partially detected	Well detected	Well detected
Cables	16	Not detected	Poorly detected	Poorly detected
Vehicles	28	Poorly detected	Partially detected	Well detected
Vertical poles	38	Not detected	Not detected	Not detected
Rooftops	14	Poorly detected	Poorly detected	Partially detected

7.2 Individual tree detection

Figure 24 presents the overall precision and recall of each ITD method with different distance thresholds. Figure 24 shows that method 3 had clearly the best overall precision with precisions ranging from 0.19 to 0.87. Method 3 was followed by method 1 with precisions ranging from 0.05 to 0.47 and method 2 with precisions ranging from 0.06 to 0.32. However, the recall measurements produced rather different results. Methods 1 and 2 performed rather similarly with recalls varying from 0.09 to 0.79 and 0.14 to 0.79 respectively, whereas the recalls of method 3 varied from 0.11 to 0.50.

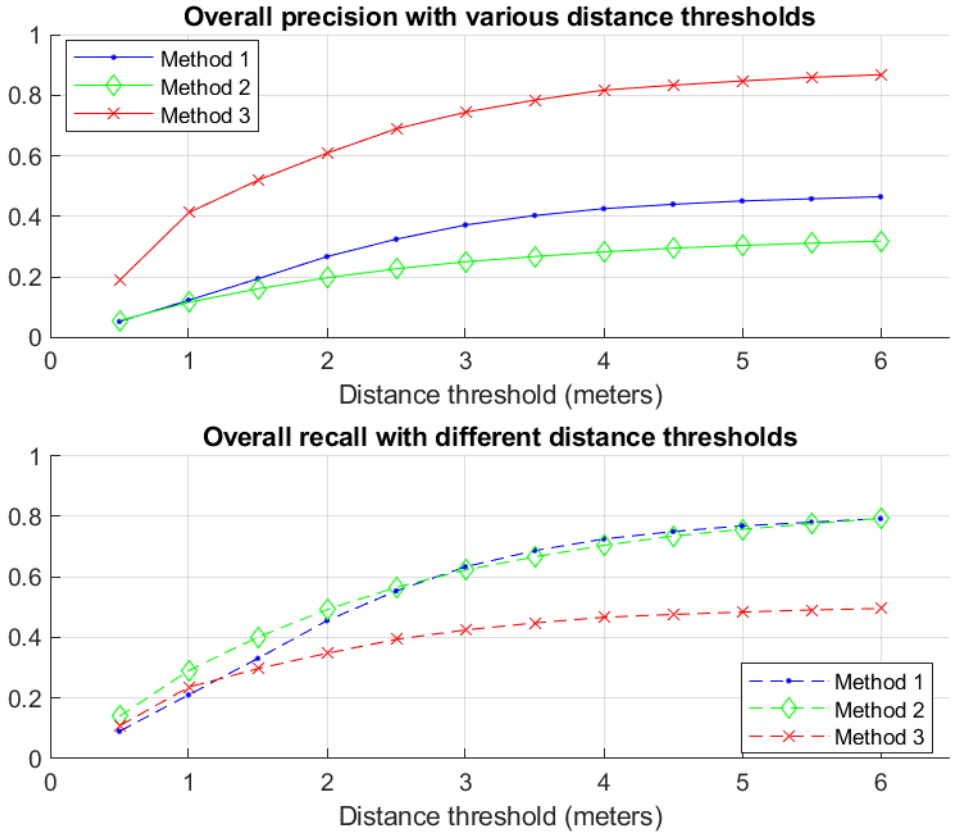

Figure 24 The overall precision and recall of each method with various distance thresholds

The performance of the ITD methods was also tested for the three most common genera separately. Figure 25 presents the recalls for the three most frequent genera – Tilia, Betula and Acer. Methods 1 and 2 detected trees belonging to the Tilia genus in a similar way (recall ranges 0.08-0.075 and 0.14-0.78 respectively), but the performance of method 3 was poorer (recall range 0.11-0.50). Method 2 was the best in detecting Betula trees, with a recall range of 0.13 to 0.91. Method 1 followed method 2 with recalls varying from 0.07 to 0.78 and method 3 performed in the poorest manner with recalls ranging from 0.08 to 0.52. Acer trees were detected in a similar manner by methods 1 and 2, with recalls ranging from 0.17 to 0.92 and 0.20 to 0.93 respectively. Method 3 was, again, the poorest performer with recalls ranging from 0.08 to 0.52.

Figure 26 shows the recalls per genus plotted by method. The figure reveals some differences in how the three genera were detected by each method. Acer had a slightly better detection

rate with method 1 than the two other genera. Method 2, in turn, detected Tilia poorer than Acer and Betula. The performance of method 3 with the various genera showed no significant differences.

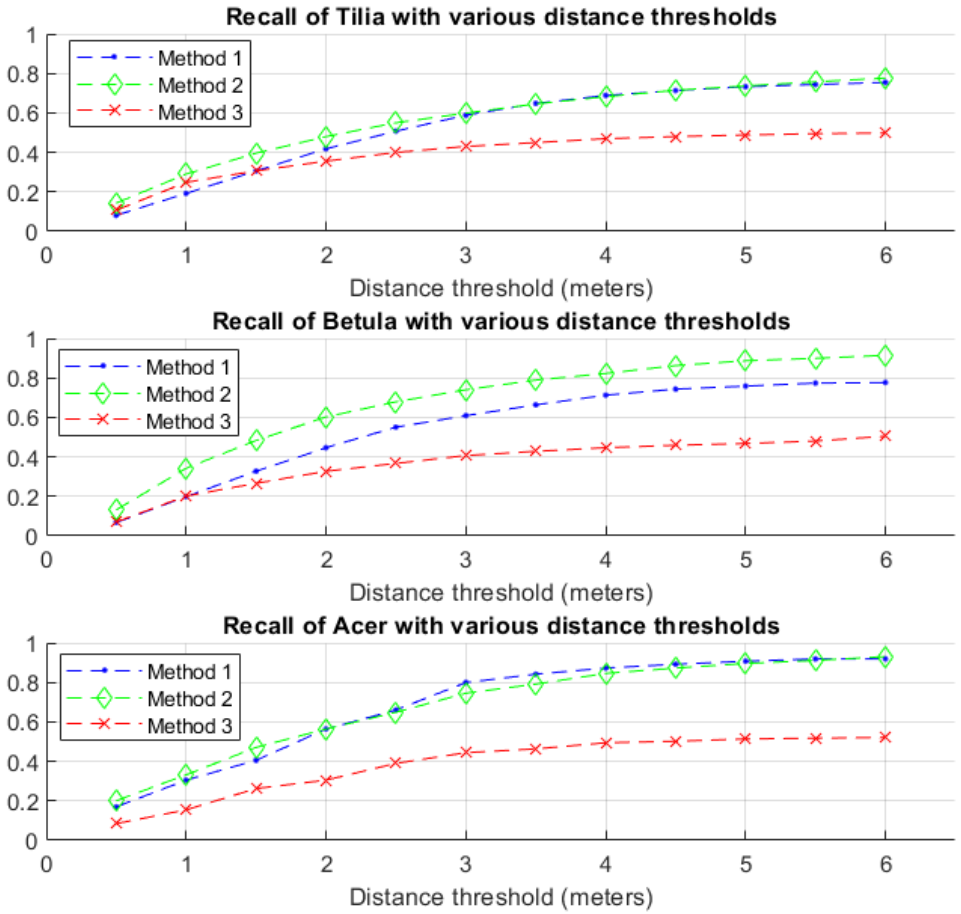

Figure 25 Recall per genus with various distance thresholds

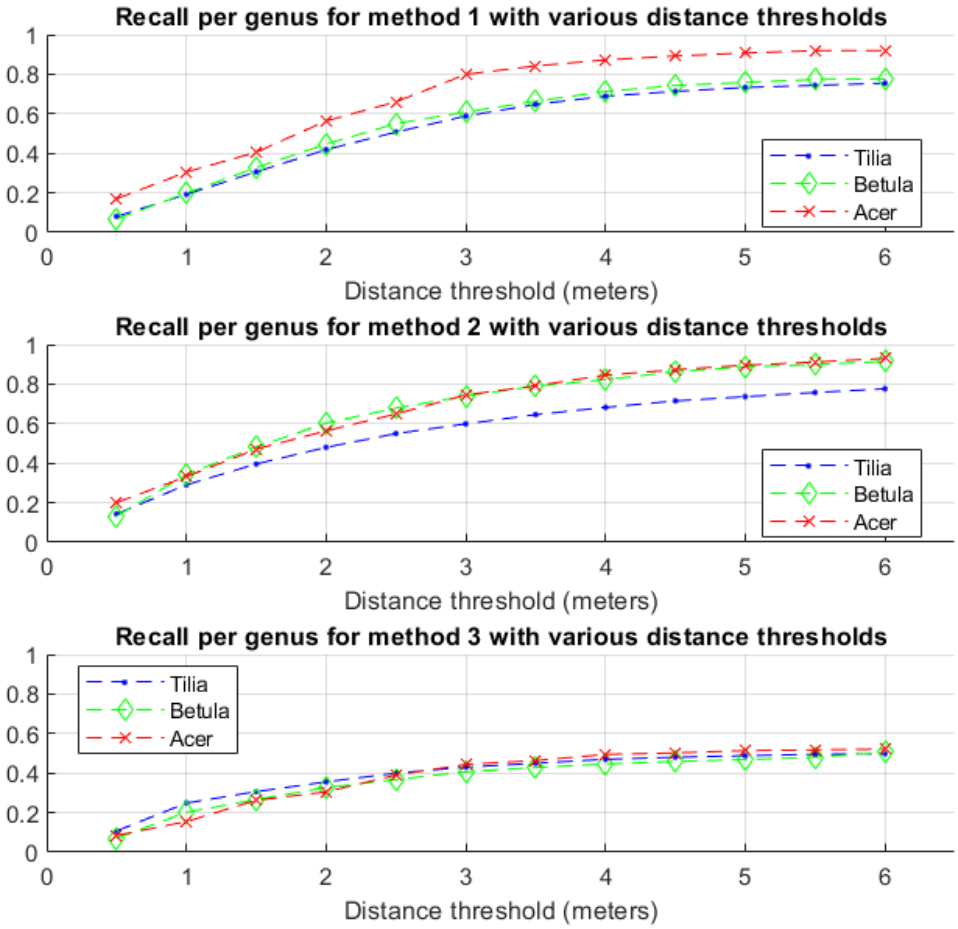

Figure 26 Recall per genus for each ITD method

The performance of the three methods was tested for five height classes separately. The height classes were under 5 metres, 5 to 10 metres, 10 to 15 metres, 15 to 20 metres and over 20 metres. Table 1 presents the recall ranges for each method and height class. Method 3 detected trees belonging to the three lowest height classes poorer than the two other methods (Figure 27). However, in the case of the two highest classes, method 3 performed similarly as the two other methods. The performance of method 3 was even slightly better with small distance thresholds.

Figure 28 presents the recalls of each height class plotted by method. The figure reveals some differences in how the trees of each height class were detected by each method. The smallest trees (height class under 5 m) were detected in the poorest manner with all three methods. However, the detection of the other height classes varied between the methods and distance thresholds. Method 1 detected trees of medium height (height classes 5 to 10 m and 10 to 15 m) best with smaller distance thresholds, but when the distance threshold increased, the detection of the larger trees (height classes 15 to 20 m and over 20 m) was similar to the detection of the medium trees. Method 2 showed a similar trend, although the difference in detection between medium and large trees was not as clear with smaller distance thresholds. The performance of method 3 was rather straightforward, as, generally, the recalls of method 3 increased, when the size of the trees increased.

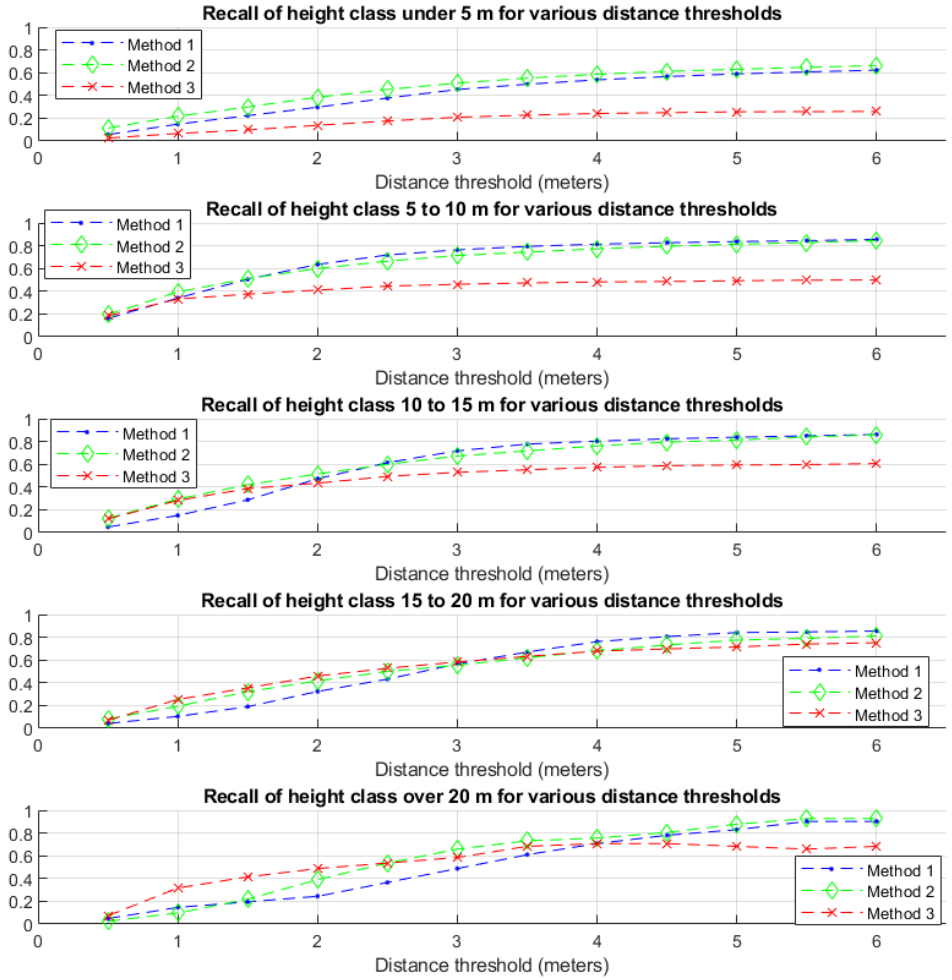

Figure 27 Recall per height with various distance thresholds

Table 6 The recall ranges of different methods and height classes

Height class	Recall range (method 1)	Recall range (method 2)	Recall range (method 3)
Under 5 m	0.06-0.62	0.11-0.66	0.03-0.26
5 to 10 m	0.16-0.86	0.20-0.85	0.18-0.50
10 to 15 m	0.05-0.86	0.13-0.86	0.12-0.61
15 to 20 m	0.04-0.85	0.08-0.81	0.07-0.75
Over 20 m	0.05-0.90	0.02-0.93	0.07-0.68

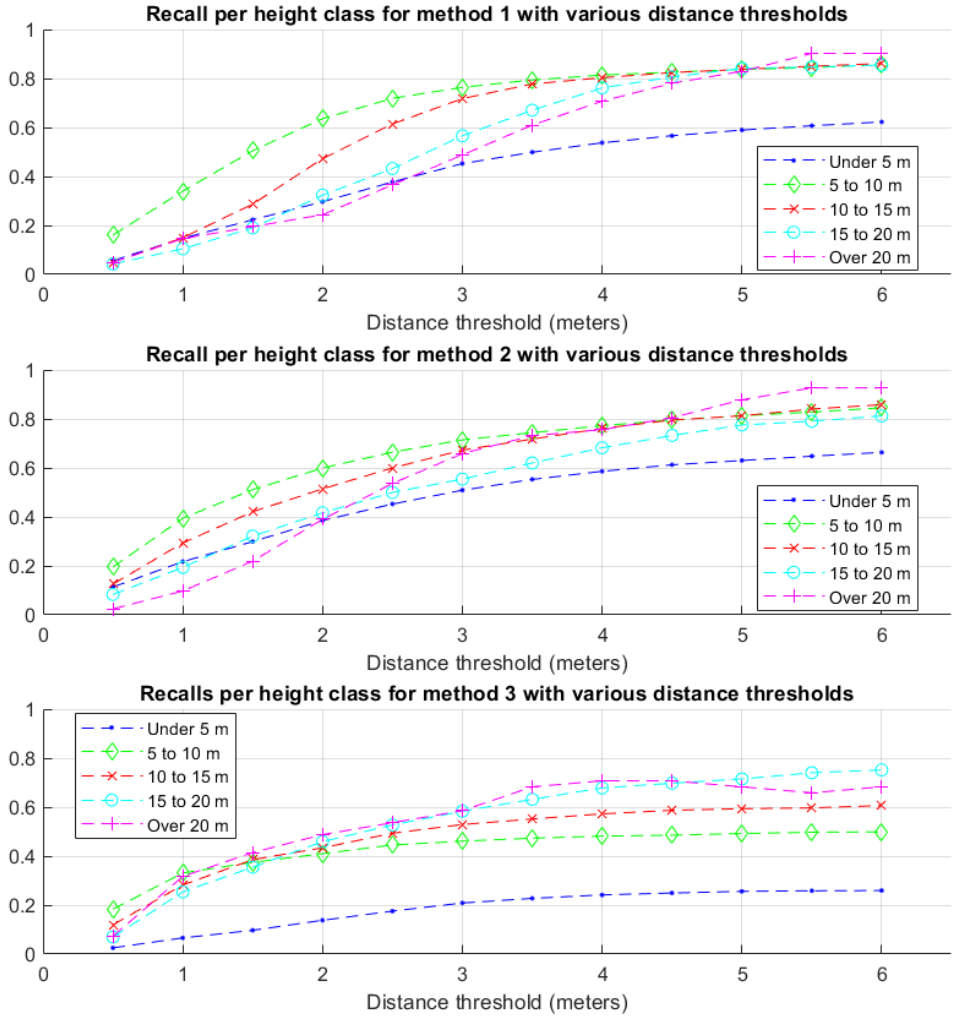

Figure 28 Recall per height for each ITD method

8 Discussion

8.1 Improving the vegetation point classification

The performance of the cleaning algorithm was based on plane searching. Thus, it is no surprise that the false vegetation points originating from flat surfaces, such as bus stops and cars, were removed most extensively. The algorithm worked most efficiently when there was a clear view to the object. The false vegetation points originating from objects that were located under trees or other objects were detected and removed poorly. This was because fewer laser pulses had reached these objects, which led to a lower point density. This resulted in larger normal vector differences between the points belonging to the object which, in turn, led to the points not being segmented together. This observation was most evident with the vehicle class. Parked cars on the side of the road were often located under trees and thus the detection of false vegetation points originating from these cars was poor. In contrast, moving cars were directly under the line-of-sight, which resulted in a more accurate detection.

Objects belonging to the cables class were detected rather poorly. This seemed to be a result of the narrowness of the objects. The laser points originating from cables were sometimes irregularly spaced, as not all parts of the cable had been hit by a laser pulse. This complicated their detection. In addition, cables were often located among trees, which further complicated their detection, as laser points belonging to cables were mixed with tree points. Furthermore, cables are not straight lines, but rather gradually turning curves. Thus, running the cleaning algorithm with a small angle threshold reduces the possibility of detecting the cables, as a small angle threshold only detects strictly planar objects. This can be seen from Figure 29, which shows the results of the cleaning algorithm with two angle thresholds. The larger angle threshold (right figure) detects a larger portion of the three cables in the sample plot than the smaller angle threshold (left figure).

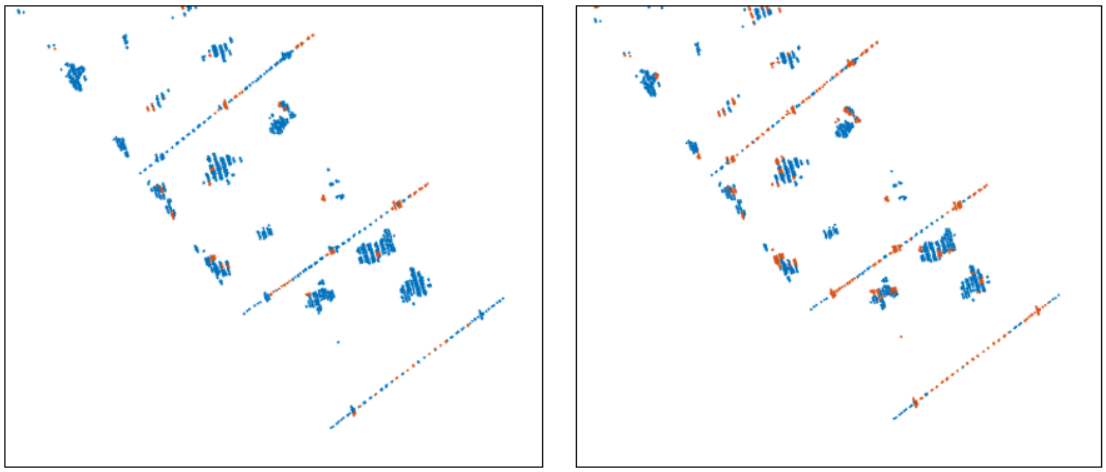

Figure 29 Two snapshots of the laser point cloud of one of the sample plots in the height range 8-10 metres. The figures present the results of the cleaning algorithm with a 5 degrees (left) and 9 degrees (right) angle threshold. The blue points are laser points classified as vegetation, whereas the orange points are points identified as false vegetation points. The three lines in the figures are airborne cables. The 9 degrees angle threshold detects a larger part of the cables than the 5 degrees angle threshold.

The cleaning algorithm was not able to detect the vertical structures, such as lamp posts and traffic signs. This was mostly a result of the narrowness of these objects, as was the case

with cables. However, the point density of these vertical structures was even smaller than the density of cables, as airborne laser scanning is a top view method that mostly detects horizontal surfaces.

The detection accuracies of all object classes, except the vertical structures class, increased when a larger angle threshold was used in the cleaning algorithm. This is rather self-evident, as a larger angle threshold allows neighbouring points with larger angular differences in their normal vectors to be segmented together. However, a larger angle threshold results in more real vegetation points to be removed from the data (Figure 30). Thus, the selection of the angle threshold is always a compromise. The angle threshold must be adjusted so that it maximises the detection of false vegetation points while minimising the removal of real vegetation points.

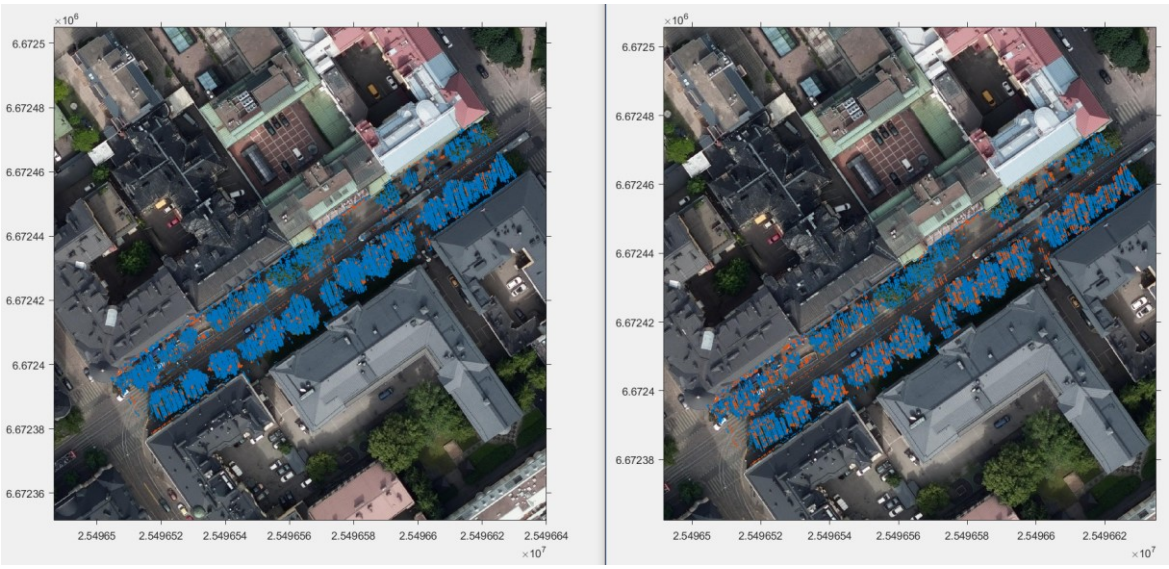

Figure 30 The result of the cleaning algorithm using angle thresholds of 5 (left) and 9 (right) degrees. Blue points are vegetation points and orange points are points that were detected as false vegetation points.

8.2 Individual tree detection

8.2.1 Limitations of the accuracy assessment

The accuracy assessment of the ITD methods measured how well the delineated tree segments could be matched with the reference trees. The matching was based on only locational similarity. Other similarity measures, such as size and shape were not considered. Thus, a tree segment that was located close to a reference tree was matched with the reference tree even though it did not resemble the tree at all. This accuracy assessment approach favoured oversegmentation, as at least one of the many oversegmented tree segments was likely to be located close to a reference tree (Figure 31).

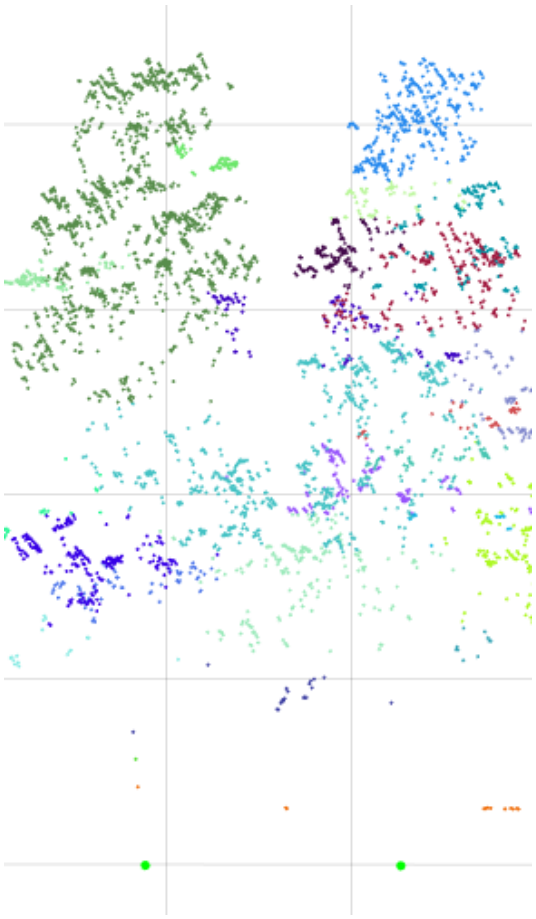

Figure 31 A side view of the point cloud containing two oversegmented trees. The laser points that are drawn with the same colour belong to the same segment. The green dots in the bottom of the figure represent the tree locations in the reference data. At least one segment in both trees is likely to match the horizontal location of the green dots.

Other issues that affected the results were related to the reference data and sample plots. Some entries of the reference data were not up to date. In addition, the locational accuracy of the entries varied. These problems were considered by manually inspecting and correcting the reference data (see chapter 6.6.2). However, even after manual correction, the reference data contained some false entries. Furthermore, the sample plots contained trees that were not in the reference data. This had a negative effect on the precisions of the ITD methods, as the methods detected trees that could not be matched with the reference data.

8.2.2 Method 1: A bottom-up approach to segment individual deciduous trees using leaf-off lidar point cloud data

Method 1 delineated the individual trees using region growing. The critical step in this region growing process was the selection of seed points. The method tried to detect stem points as points with a high intensity value and then grow the trees around these stem points. However, laser returns originating from large branches had similar intensity values as the stem returns which resulted in the stem points being scattered all around the tree canopy (Figure 32). Thus, as the region growing was performed in a bottom-up manner, the success of the delineation depended largely on where the bottom-most stem point of each tree happened to be located. If the bottom-most stem point was located close to the centre of the tree, the

delineation was successful, but if the bottom-most stem point was located close to the border of the tree, the delineation was unsuccessful. The latter case resulted in some trees being segmented into several segments and parts of neighbouring trees being segmented together (Figure 33). The method could be improved by either using additional criteria to detect the stems, or inverting the region growing process by using tree tops as seed points.

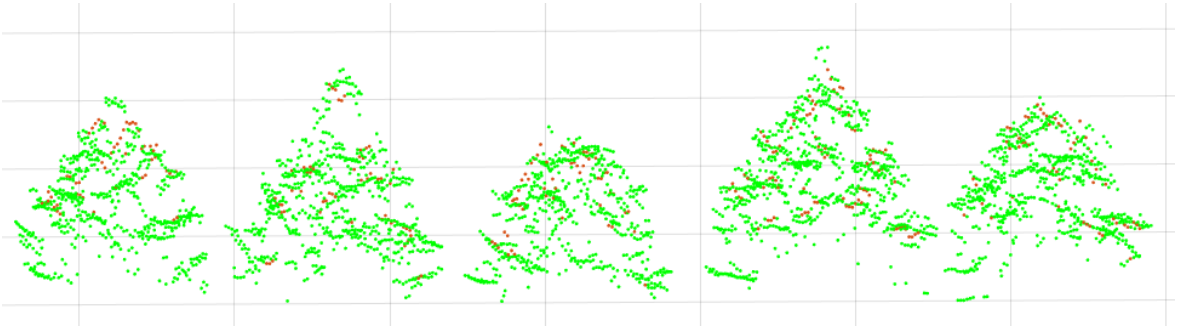

Figure 32 A side view of the laser points of five trees. The points have been divided into stem points (brown) and non-stem points (green) based on an intensity threshold. However, the stem points are scattered all around the tree canopy indicating that the separation was not successful.

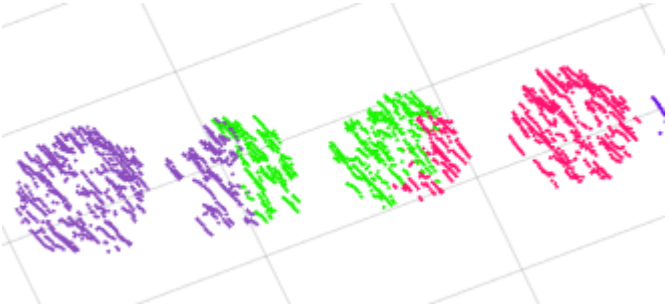

Figure 33 A top view of four trees. The bottom-most stem points were located close to the borders of the trees and thus parts of different trees were segmented together.

Another challenge with method 1 was the selection of a suitable horizontal threshold. The horizontal threshold should be chosen based on the average crown radius and average separation of the trees. Too small a threshold leads to oversegmentation (Figure 34), whereas too large a threshold leads to undersegmentation. The original method by Lu et al. (2014), to which method 1 was based on, was tested in rather homogeneous conditions. Thus, a single threshold, which was selected by trial and error, could be used for the whole study area. However, the average crown radius and separation of the trees differed significantly in the various sample plots of this study and thus the threshold had to be defined for each sample plot separately. The horizontal threshold of each sample plot was calculated with equation 5. The idea behind equation 5 was that when the separation between trees is smaller, the distances between the vegetation points in the sample plot are smaller on average. The median was used instead of mean, as the tree formations differed between the sample plots. For example, the trees were located in the middle of a street in some plots and on other sides of a street in others (Figure 35). In the latter case, the mean distance between the vegetation points was larger than in the former case, whereas the median distances did not differ by that much.

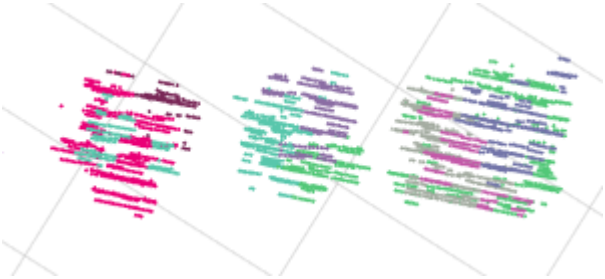

Figure 34 A top view of three trees. The chosen horizontal threshold was too small, which resulted in oversegmentation of the trees.

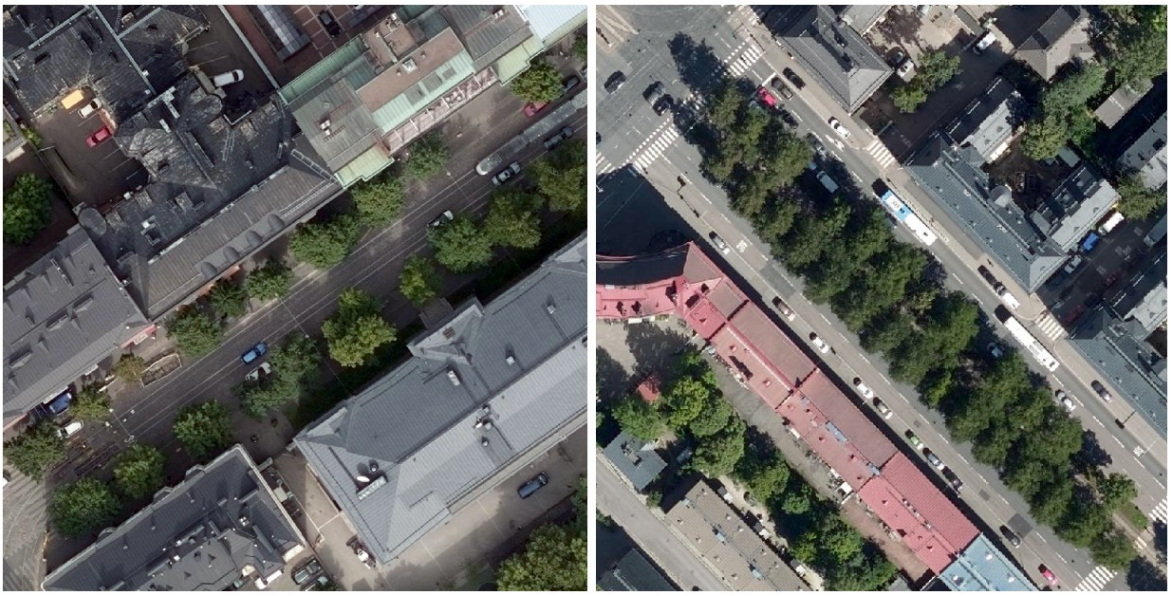

Figure 35 Two common tree formations in the sample plots. The trees are located on both sides of a street (left) or in the middle of a street (right).

Although equation (5) enabled selecting the horizontal threshold automatically, its performance was suboptimal. This resulted in oversegmentation and undersegmentation in some sample plots. Thus, method 1 could be improved by estimating the value of the optimal horizontal threshold in some other way. Pre-existing information of the tree locations, heights and DBHs could be useful in determining the threshold. Although this information was available, it was not used in this study, as the aim of the study was to create methods that work without any prerequisite knowledge.

8.2.3 Method 2: A new procedure for identifying single trees in understory layer using discrete lidar data

Method 2 contained two steps that were critical to the tree delineation process. The most critical step was determining the optimal number of clusters in each slice, as k-means clustering requires a predefined number of clusters. Several methods were tested for this task, including the Davies-Bouldin index (see Davies & Bouldin 1979), the Calinski-Harabasz index (see Caliński & Harabasz 1974), the silhouette method (see Rousseeuw 1987) and the elbow method (see e.g. Bholowalia & Kumar 2014). Common to all these methods was that they all clustered the data with various numbers of clusters and selected the optimal number of clusters based on some optimality criteria. The optimality criteria differed between each method. The elbow method was selected as the final method for

determining the optimal number of clusters, although it tended to oversegment the slices. Method 2 could most likely be improved by using a clustering method that does not require a predefined number of clusters.

The second step that had a large effect on the performance of method 2 was merging the clusters of consecutive slices. This was done by comparing the overlaps of horizontal convex hull polygons of each cluster. The problem was that many clusters contained outlier points that distorted the shape of the convex hull polygons. These outlier points were mostly false vegetation points that were not removed by the cleaning algorithm. The distortion of the convex hull polygon increased its area, which affected the merging process in two ways. Some clusters were merged, although they were not supposed to be merged and vice versa. (Figure 36). The suboptimal performance of the initial clustering amplified the problem. The problem was addressed by detecting and removing some of the outlier points of each cluster with statistical testing before creating the convex hull polygons. However, this only improved the performance of the method slightly.

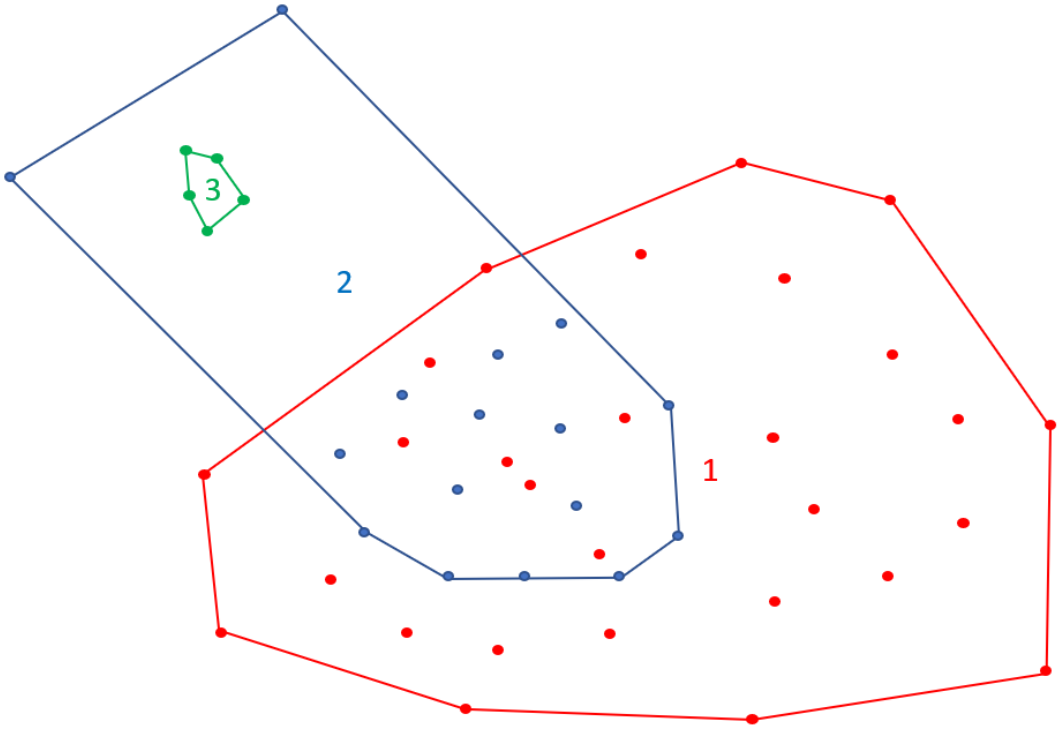

Figure 36 The cluster merging problem. Clusters 1, 2 and 3 all belong to different slices. Cluster 2 contains two outlier points that distort the convex hull polygon. As a result, cluster 2 is not merged with cluster 1, as the overlap of the two clusters is too small. Without the outlier points, the two clusters would be merged, as the overlap would be 100 %. In contrast, cluster 3 is merged with cluster 2, as it completely overlaps with the distorted part of the polygon of cluster 2.

Method 2 produced largely oversegmented trees. This is a result of the poor initial clustering and the problematic merging of clusters in different slices. The recalls calculated for method 2 give a rather misleading insight on the performance of the method, as the accuracy assessment favours oversegmentation (see chapter 8.2.1).

8.2.4 Method 3: An efficient, multi-layered crown delineation algorithm for mapping individual tree structure across multiple ecosystems

Method 3 had the highest precision, but the lowest recall of the three ITD methods. This indicates that method 3 undersegmented the trees. The undersegmentation of trees is rather evident when inspecting the results of the tree delineations of the sample plots (Figure 37).

Figure 37 A top view of the delineation of a sample plot. The undersegmentation of trees is rather evident.

Undersegmentation occurred especially when the tree separation was small, as this complicated the performance of the marker-controlled watershed algorithm. The algorithm segmented the vegetation points using local maxima (tree tops) and inverse "ridge lines" (areas between trees) of the raster canopy height model. The local maxima and inverse ridge lines were both highlighted from the CHM with morphological operators. A small tree separation resulted in some local maxima and ridge lines not being detected which, in turn, resulted in undersegmentation.

Another variable that affected the performance of method 3 was tree height. Method 3 had difficulties detecting small trees (Figure 28). Small trees were often surrounded by larger trees and other higher objects. Thus, their tree tops were not the highest points in their neighbourhood (i.e. local maxima) and the tree tops were not detected. This, in turn, resulted in the trees not being detected.

Method 3 was supposed to be able to detect understory trees. However, the sample plots used in this study contained almost no understory trees, so the understory tree detection was not really tested. Most understory trees detected in the sample plots were in reality parts of the overstory tree, as shown in Figure 38.

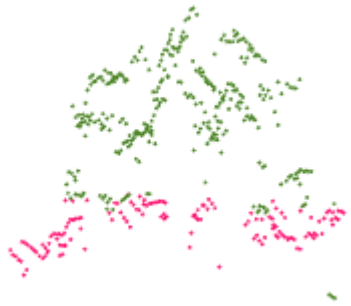

Figure 38 One tree mistakenly detected as an understory and overstory tree.

8.2.5 Comparison of methods

The overall precision of method 3 was significantly better than the overall precisions of methods 1 and 2 (Figure 24). In contrast, the overall recalls of methods 1 and 2 were significantly better than the overall recall of method 3. These results were due to method 3's tendency to undersegment the trees and method 1 and 2's tendency to oversegment the trees. The results suggest that method 3 delineates the trees more accurately, whereas the other two methods detect a larger portion of the trees. However, the numerical results do not represent the whole truth. As mentioned in chapter 8.2.3, the recalls of method 2 are rather optimistic, as most applications of ITD would require the delineated tree to resemble its real counterpart to at least some extent.

Methods 2 and 3 give satisfactory results when there is a clear separation between trees. However, their performance is hindered when the separation becomes smaller, as this complicates the cluster detection of method 2, and the local maxima and inverse ridge line detection of method 3. A small tree separation also affects the performance of method 1, but not by that much. Thus, method 1 is the best choice, if no pre-existing knowledge of the tree locations or crown sizes is available.

The genus specific measures provided rather similar results as the overall measures (Figure 25). Method 2 detected Betula trees slightly better than method 1, but otherwise the performance of these two methods was almost identical. In contrast, method 3's ability to detect trees of all three genera was clearly inferior to the other two methods. Based on these results, either method 1 or 2 is the suggested method when delineating trees of the three tested genera.

The height specific measures provided slightly different results than the overall and genus specific measures. Again, methods 1 and 2 provided superior results to method 3 with smaller trees (Figure 27). However, the performance of method 3 increased with respect to the other two methods, when the tree height increased. Method 3 performed similarly as the other two methods with the second largest height class and with the largest height class, its performance was superior to the other two methods with small distance thresholds. This phenomenon is most likely a result of the way in which the seed points or starting locations for the delineation were determined. Method 3 is the only method where the delineation is performed in a top-down manner, as the local maxima in the CHM represent tree tops to which all lower parts of the trees are segmented. When the tree height is small, method 3 has problems detecting the tree tops, but as the tree height increases, the tree top detection

becomes more successful. The successful detection of the tree tops, in turn, results in a better detection rate. Thus, method 3 is a suitable tree delineation method when the tree heights are large, but otherwise one of the other two ITD methods is preferred.

8.2.6 Comparison to previous studies

Many cities and municipalities keep a register of urban trees that are located within the limits of the city or municipality. Urban tree registers enable matching the tree segments delineated with ITD methods with the trees in the register. Thus, the detection rate (i.e. recall) is a more important measure than precision, as false tree segments can be removed, when the number and location of the trees is known beforehand. As a result, most studies concerning urban ITD only report the detection rate. Comparing the detection rates, or recalls, of this study to other similar studies reveals that the three ITD methods tested need improvements. For example, Tanhuanpää et al. (2014) and Liu et al. (2013) reached detection rates of over 85 %. Tanhuanpää et al. detected 88.8 % of street trees using a surface model-based watershed segmentation method. They detected a match between a reference tree and tree segment if the location of the reference tree was within the tree segment. However, if more than one reference trees were located within the same tree segment, none of these reference trees were defined as detected. The detection rates of Liu et al. (2013) varied from 85.4 % to 86.8 %. They calculated the detection rate using visual inspection. The results of these two studies are not directly comparable to the results of this study, as the methods used for determining the detection rate were somewhat different. Holopainen et al. (2013b) detected 65.5 % of urban park trees using a marked watershed segmentation algorithm. In their study, a reference tree was defined as detected, if the closest tree segment was located within 4 metres of the reference tree. Thus, the detection rate of the study by Holopainen et al. (2013b) is almost directly comparable with the results of this study when using a 4 metres distance threshold. With this distance threshold, methods 1,2 and 3 produced detection rates of 72.5 %, 70.3 % and 46.6 %, respectively (Figure 24). The values of methods 1 and 2 are in the same range as the detection rate of Holopainen et al. (2013b). However, the detection rate of method 2 gives a rather misleading image of the method's performance, as the method produces largely oversegmented trees.

9 Conclusions

The fundamental challenge of urban ALS-based individual tree detection is the correct classification of vegetation points, as falsely classified vegetation points affect the tree delineation in a major way. Classification based on elevation is not a sufficient method for extracting the vegetation points, as urban environments contain a wide variety of objects that create laser returns on the same height range as trees. Thus, additional classification methods, such as grouping and region growing should be applied to detect the various man-made objects of an urban environment.

This study tested a region growing-based plane searching algorithm that detected and removed false vegetation points. The performance of this "cleaning" algorithm was far from optimal. The algorithm was most suitable for larger flat objects, but the detection of narrow and irregularly shaped objects was very poor. However, the removal of even a portion of the false vegetation points improves the tree delineation and thus the algorithm has some potential. The false vegetation point removal could be improved by optimising the parameters of the algorithm and using it together with other algorithms that specialise on narrow and irregular objects. The development of these algorithms is a potential subject for further studies concerning urban individual tree detection.

This study tested three methods for detecting individual trees in urban environments. The performance of each method was strongly affected by the false vegetation points in the point cloud data. This observation further confirms the importance of an accurate classification of the vegetation points. In addition to the vegetation point classification, the single most effective step in the tree delineation process was the determination of the seed points or starting locations of the delineation. There was a strong dependency between the detection of a suitable seed point/starting location and the success of the delineation. A suitable starting location for the delineation is somewhere close to the horizontal centre of a tree. Method 1 utilised this observation and delineated the trees using the laser points originating from tree stems as the seed points. The problem with this was that the detection of stem points proved to be challenging. A more easily detectable starting point for the delineation could be the tree top, although tree top detection is not a trivial task, as was shown by method 3. Another possible way of determining the starting points could be using pre-existing tree location information, which is often available in tree registers kept by cities and municipalities.

Method 1 was the best overall performer of the three tested methods. Its performance was the most robust with varying conditions. The performance of the method was hindered by the poor detection of stem points. Thus, the method could be improved by determining the seed points in another way, such as detecting the tree tops. This task could be performed using a surface model method similar to method 3. This would also mean that the delineation of trees would be top-down rather than bottom-up. This, in turn, would require inverting the region growing process of method 1. However, this should not be too challenging a task. Thus, based on the results and observations acquired in this study, the optimal ITD method for urban environments would be a combination of methods 1 and 3.

References

Ardila, J.P., Bijker, W., Tolpekin, V.A. & Stein, A. (2012) Context-sensitive extraction of tree crown objects in urban areas using VHR satellite images. *International Journal of Applied Earth Observations and Geoinformation.* Vol. 15. p. 57-69. ISSN 0303-2434.

Baltsavias, E.P. (1999) Airborne laser scanning: basic relations and formulas. *ISPRS Journal of Photogrammetry and Remote Sensing.* Vol. 54:2-3. p. 199-214. ISSN 0924-2716.

Bholowalia, P. & Kumar, A. (2014) EBK-Means: A Clustering Technique based on Elbow Method and K-Means in WSN. *International Journal of Computer Applications.* Vol. 105:9. p. 17-24. ISSN 0975-8887.

Bolund, P. & Hunhammar, S. (1999) Ecosystem services in urban areas. *Ecological Economics.* Vol. 29:2. p. 293-301. ISSN 0921-8009.

Budei, B.C., St-Onge, B., Hopkinson, C. & Audet, F. (2018) Identifying the genus or species of individual trees using a three-wavelength airborne lidar system. *Remote sensing of environment.* Vol. 204. p. 632-647. ISSN 0034-4257.

Caliński, T. & Harabasz, J. (1974) A dendrite method for cluster analysis. *Communications in Statistics-theory and Methods.* Vol. 3:1. p. 1-27. ISSN 0361-0926.

Chacalo, A., Aldama, A. & Grabinsky, J. (1994) Street tree inventory in Mexico City. *Journal of Arboriculture.* Vol. 20. p. 222-226. ISSN 0278-5226.

Chen, Q., Baldocchi, D., Gong, P. & Kelly, M. (2006) Isolating individual trees in a Savanna woodland using small footprint LiDAR data. *Photogrammetric Engineering & Remote Sensing.* Vol. 72:8. p. 923-932. ISSN 0099-1112.

Daily, G. (1997) *Natures services: societal dependence on natural ecosystems.* Washington DC, USA: Island Press. 412 p. ISBN 1-55963-475-8.

Davies, D.L. & Bouldin, D.W. (1979) A Cluster Separation Measure. *IEEE Transactions on Pattern Analysis and Machine Intelligence.* Vol. PAMI-1:2. p. 224-227. ISSN 0162-8828.

Denk, W., Strickler, J.H. & Webb, W.W. (1990) Two-photon laser scanning fluorescence microscopy. *Science.* Vol. 248:4951. p. 73-76. ISSN 1095-9203.

Duncanson, L.I., Cook, B.D., Hurtt, G.C. & Dubayah, R.O. (2014) An efficient, multi-layered crown delineation algorithm for mapping individual tree structure across multiple ecosystems. *Remote Sensing of Environment.* Vol. 154. p. 378-386. ISSN 0034-4257.

Ferraz, A., Bretar, F., Jacquemoud, S., Gonçalves, G., Pereira, L., Tomé, M. & Soares, P. (2012) 3-D mapping of a multi-layered Mediterranean forest using ALS data. *Remote Sensing of Environment.* Vol. 121. p. 210-223. ISSN 0034-4257.

Höfle, B., Hollaus, M. & Hagenauer, J. (2012) Urban vegetation detection using radiometrically calibrated small-footprint full-waveform airborne LiDAR data. *ISPRS Journal of Photogrammetry and Remote Sensing.* Vol. 67. p. 134-147. ISSN 0924-2716.

Holopainen, M., Hyyppä, J. & Vastaranta, M. (2013a) *Laserkeilaus metsävarojen hallinnassa.* 5 edn. Helsinki, Finland: Univ. of Helsinki. 75 p. ISBN 978-952-10-4533-2.

Holopainen, M., Kankare, V., Vastaranta, M., Liang, X., Lin, Y., Vaaja, M., Yu, X., Hyyppä, J., Hyyppä, H., Kaartinen, H., Kukko, A., Tanhuanpää, T. & Alho, P. (2013b) Tree mapping using airborne, terrestrial and mobile laser scanning – A case study in a heterogeneous urban forest. *Urban Forestry & Urban Greening.* Vol. 12:4. p. 546-553. ISSN 1618-8667.

Hyyppä, J. & Inkinen, M. (1999) Detecting and estimating attributes for single trees using laser scanner. *The Photogrammetric Journal of Finland.* Vol. 16. p. 27-42. ISSN 0554-1069.

Hyyppä, J., Kelle, O., Lehikoinen, M. & Inkinen, M. (2001) A segmentation-based method to retrieve stem volume estimates from 3-D tree height models produced by laser scanners. *IEEE Transactions on Geoscience and Remote Sensing.* Vol. 39:5. p. 969-975. ISSN 0196-2892.

Jaakkola, A., Hyyppä, J., Kukko, A., Yu, X., Kaartinen, H., Lehtomäki, M. & Lin, Y. (2010) A low-cost multi-sensoral mobile mapping system and its feasibility for tree measurements. *ISPRS Journal of Photogrammetry and Remote Sensing.* Vol. 65:6. p. 514-522. ISSN 0924-2716.

Jutras, P., Prasher, S.O. & Mehuys, G.R. (2009) Prediction of street tree morphological parameters using artificial neural networks. *Computers and Electronics in Agriculture.* Vol. 67:1-2. p. 9-17. ISSN 0168-1699.

Kaartinen, H., Hyyppä, J., Yu, X., Vastaranta, M., Hyyppä, H., Kukko, A., Holopainen, M., Heipke, C., Hirschmugl, M., Morsdorf, F., Næsset, E., Pitkänen, J., Popescu, S., Solberg, S., Wolf, B.M. & Wu, J. (2012) An International Comparison of Individual Tree Detection and Extraction Using Airborne Laser Scanning. *Remote Sensing.* Vol. 4:4. p. 950-974. ISSN 2072-4292.

Kandare, K., Dalponte, M., Gianelle, D. & Chan, J.C.W. (2014) A new procedure for identifying single trees in understory layer using discrete lidar data. *Ieee International Geoscience and Remote Sensing Symposium.* 2014. New York. IEEE International. p. 1357-1360.

Keller, J.K. & Konijnendijk, C.C. (2012) A comparative analysis of municipal urban tree inventories of selected major cities in North America and Europe. *Arboriculture & Urban Forestry.* Vol. 38:1. p. 24-30. ISSN 1935-5297.

Konijnendijk, C., Nilsson, K., Randrup, T.B. & Schipperijn, J. (2005) *Urban Forests and Trees.* 1 edn. Heidelberg, Germany: Springer-Verlag Berlin Heidelberg. 520 p. ISBN 978-3-540-27684-5.

Kukko, A., Kaartinen, H., Hyyppä, J. & Chen, Y. (2012) Multiplatform Mobile Laser Scanning: Usability and Performance. *Sensors.* Vol. 12:9. p. 11712-11733. ISSN 1424-8220.

Lang, S., Tiede, D., Maier, B. & Blaschke, T. (2006) 3D Forest structure analysis from optical and LIDAR data / Análise 3D da estrutura da floresta com dados ópticos e da LIDAR. *Ambiência.* Vol. 2:3. p. 95-110. ISSN 2175-9405.

Lee, H., Slatton, K.C., Roth, B.E. & Cropper Jr, W.P. (2010) Adaptive clustering of airborne LiDAR data to segment individual tree crowns in managed pine forests. *International Journal of Remote Sensing.* Vol. 31:1. p. 117-139. ISSN 1366-5901.

Li, W., Guo, Q., Jakubowski, M.K. & Kelly, M. (2012) A new method for segmenting individual trees from the lidar point cloud. *Photogrammetric Engineering & Remote Sensing.* Vol. 78:1. p. 75-84. ISSN 0099-1112.

Lindberg, E., Eysn, L., Hollaus, M., Holmgren, J. & Pfeifer, N. (2014) Delineation of Tree Crowns and Tree Species Classification From Full-Waveform Airborne Laser Scanning Data Using 3-D Ellipsoidal Clustering. *IEEE Journal of Selected Topics in Applied Earth Observations and Remote Sensing.* Vol. 7:7. p. 3174-3181. ISSN 1939-1404.

Lindberg, E., Briese, C., Doneus, M., Hollaus, M., Schroiff, A. & Pfeifer, N. (2015) Multi-wavelength airborne laser scanning for characterization of tree species. In. Durrieu, S. and Véga, C., eds. *SilviLaser 2015.* La Grande-Motte, France. 28th-30th September 2015. Saint-Mandé Cedex, France. p. 271-273.

Lindberg, E. & Holmgren, J. (2017) Individual Tree Crown Methods for 3D Data from Remote Sensing. *Current Forestry Reports.* Vol. 3:1. p. 19-31. ISSN 2198-6436.

Liu, J., Shen, J., Zhao, R. & Xu, S. (2013) Extraction of individual tree crowns from airborne LiDAR data in human settlements. *Mathematical and Computer Modelling.* Vol. 58:3-4. p. 524-535. ISSN 1872-9479.

Lu, X., Guo, Q., Li, W. & Flanagan, J. (2014) A bottom-up approach to segment individual deciduous trees using leaf-off lidar point cloud data. *ISPRS Journal of Photogrammetry and Remote Sensing.* Vol. 94. p. 1-12. ISSN 0924-2716.

Lyytimäki, J., Petersen, L.K., Normander, B. & Bezák, P. (2008) Nature as a nuisance? Ecosystem services and disservices to urban lifestyle. *Environmental Sciences.* Vol. 5:3. p. 161-172. ISSN 1569-3430.

MathWorks. (2018) Marker-Controlled Watershed Segmentation. mathworks.com. [Online]. Available: https://se.mathworks.com/help/images/marker-controlled-watershed-segmentation.html [Accessed: 15.10. 2018].

Milonni, P.W. & Eberly, J.H. (2010) *Laser Physics.* Hoboken, New Jersey, USA: John Wiley & Sons, Incorporated. 831 p. ISBN 978-0-470-38771-9.

Mongus, D. & Žalik, B. (2015) An efficient approach to 3D single tree-crown delineation in LiDAR data. *ISPRS Journal of Photogrammetry and Remote Sensing.* Vol. 108. p. 219-233. ISSN 0924-2716.

Morsdorf, F., Meier, E., Allgöwer, B. & Nüesch, D. (2003) Clustering in airborne laser scanning raw data for segmentation of single trees. *International Archives of the Photogrammetry, Remote Sensing and Spatial Information Sciences.* Vol. 34:part 3. p. W13. ISSN 2194-9034.

Naesset, E. (1997) Determination of mean tree height of forest stands using airborne laser scanner data. *ISPRS Journal of Photogrammetry & Remote Sensing.* Vol. 52:2. p. 49-56. ISSN 0924-2716.

Næsset, E. (2002) Predicting forest stand characteristics with airborne scanning laser using a practical two-stage procedure and field data. *Remote Sensing of Environment.* Vol. 80:1. p. 88-99. ISSN 0034-4257.

Nielsen, A.B., Östberg, J. & Delshammar, T. (2014) Review of urban tree inventory methods used to collect data at single-tree level. *Arboriculture & Urban Forestry.* Vol. 40:2. p. 96-111. ISSN 1935-5297.

Nowak, D.J., Crane, D.E. & Stevens, J.C. (2006) Air pollution removal by urban trees and shrubs in the United States. *Urban Forestry & Urban Greening.* Vol. 4:3-4. p. 115-123. ISSN 1618-8667.

Oksanen, J. (2012) Digital Elevation Model. maanmittauslaitos.fi. [Online]. Available: http://www.maanmittauslaitos.fi/en/research/interesting-topics/digital-elevation-model [Accessed: 16.3. 2018].

Persson, Å, Holmgren, J. & Söderman, U. (2002) Detecting and measuring individual trees using an airborne laser scanner. *Photogrammetric Engineering And Remote Sensing.* Vol. 68:9. p. 925-932. ISSN 0099-1112.

Rabbani, T., van den Heuvel, F. A, Vosselman, G., Maas, H.G. & Schneider, D. (2006) Segmentation of point clouds using smoothness constraints. In. Maas, H.G. and Schneider, D., eds. *ISPRS Commission V Symposium 'Image Engineering and Vision Metrology'.* Dresden, Germany. 25th-27th September 2006. Dresden, Germany. International Society for Photogrammetry and Remote Sensing (ISPRS). p. 248-253.

Reitberger, J., Schnörr, C., Krzystek, P. & Stilla, U. (2009) 3D segmentation of single trees exploiting full waveform LIDAR data. *ISPRS Journal of Photogrammetry and Remote Sensing.* Vol. 64:6. p. 561-574. ISSN 0924-2716.

Rousseeuw, P.J. (1987) Silhouettes: a graphical aid to the interpretation and validation of cluster analysis. *Journal of computational and applied mathematics.* Vol. 20. p. 53-65. ISSN 0377-0427.

Straub, B. (2003) A Top-Down Operator For the Automatic Extraction of Trees - Concept and Performance Evaluation. *Proceedings of the ISPRS Working Group III/3 Workshop*

*3-D Reconstruction from Airborne Laser Scanner and InSAR data * Dresden, Germany. 8th-10th October 2003. p. 34-39.

Tang, S., Dong, P. & Buckles, B.P. (2013) Three-dimensional surface reconstruction of tree canopy from lidar point clouds using a region-based level set method. *International Journal of Remote Sensing.* Vol. 34:4. p. 1373-1385. ISSN 0143-1161.

Tanhuanpää, T., Vastaranta, M., Kankare, V., Holopainen, M., Hyyppä, J., Hyyppä, H., Alho, P. & Raisio, J. (2014) Mapping of urban roadside trees – A case study in the tree register update process in Helsinki City. *Urban Forestry & Urban Greening.* Vol. 13:3. p. 562-570. ISSN 1618-8667.

Tanhuanpää, T. (2016) *Developing laser scanning applications for mapping and monitoring single tree characteristics for the needs of urban forestry.* Doctoral thesis. University of Helsinki. Helsinki, Finland.

Teledyne Optech. (2015) Optech Titan Multispectral Lidar System. Teledyneoptech.com. [Online]. Available: http://www.teledyneoptech.com/wp-content/uploads/Titan-Specsheet-150515-WEB.pdf [Accessed: 24.5. 2018].

Vastaranta, M., Kankare, V., Holopainen, M., Yu, X., Hyyppä, J. & Hyyppä, H. (2012) Combination of individual tree detection and area-based approach in imputation of forest variables using airborne laser data. *ISPRS Journal of Photogrammetry and Remote Sensing.* Vol. 67. p. 73-79. ISSN 0924-2716.

Véga, C. & Durrieu, S. (2011) Multi-level filtering segmentation to measure individual tree parameters based on Lidar data: Application to a mountainous forest with heterogeneous stands. *International Journal of Applied Earth Observations and Geoinformation.* Vol. 13:4. p. 646-656. ISSN 0303-2434.

Vosselman, G. & Maas, H. (2010) *Airborne and Terrestrial Laser Scanning.* Dunbeath, Caithness, Scotland, UK: Whittles Publishing. 336 p. ISBN 978-1-62870-092-3.

Wallace, L., Musk, R. & Lucieer, A. (2014) An Assessment of the Repeatability of Automatic Forest Inventory Metrics Derived From UAV-Borne Laser Scanning Data. *IEEE Transactions on Geoscience and Remote Sensing.* Vol. 52:11. p. 7160-7169. ISSN 0196-2892.

Wehr, A. & Lohr, U. (1999) Airborne laser scanning—an introduction and overview. *ISPRS Journal of Photogrammetry and Remote Sensing.* Vol. 54:2. p. 68-82. ISSN 0924-2716.

Yao, W. & Wei, Y. (2013) Detection of 3-D Individual Trees in Urban Areas by Combining Airborne LiDAR Data and Imagery. *IEEE Geoscience and Remote Sensing Letters.* Vol. 10:6. p. 1355-1359. ISSN 1545-598X.

Yu, X., Hyyppä, J., Vastaranta, M., Holopainen, M. & Viitala, R. (2011) Predicting individual tree attributes from airborne laser point clouds based on the random forests

technique. *ISPRS Journal of Photogrammetry and Remote Sensing.* Vol. 66:1. p. 28-37. ISSN 0924-2716.

Zhang, C., Zhou, Y. & Qiu, F. (2015) Individual Tree Segmentation from LiDAR Point Clouds for Urban Forest Inventory. *Remote Sensing.* Vol. 7:6. p. 7892-7913. ISSN 2072-4292.

Appendices

Appendix 1. Example of a confusion matrix. 1 page.

Appendix 1. Example of a confusion matrix

The following table presents an example confusion matrix. The example confusion matrix presents the results of method 1 when a distance threshold of 2 metres was used. Not all columns of the confusion matrix are included in the example, as the whole matrix would not fit on the page. Note that the values in the No tree column are very large. This means that there were many delineated trees for which a matching reference tree was not found. These false trees are a result of two phenomena. Firstly, the non-tree objects that were not removed by the cleaning algorithm have been interpreted as trees and secondly, the method has oversegmented the trees.

	No tree	Acer under 5 m	Acer 5 to 10 m	Acer 10 to 15 m	Acer 15 to 20 m	Acer over 20 m	Betula under 5 m	Betula 5 to 10 m	Betula 10 to 15 m	Betula 15 to 20 m	Betula over 20 m
No tree	0	10	27	51	25	0	47	24	40	55	15
Tree under 5 m	226	0	0	0	0	0	0	0	0	0	0
Tree 5 to 10 m	1001	5	56	1	0	0	0	2	0	1	0
Tree 10 to 15 m	1518	3	17	31	2	0	4	8	22	2	0
Tree 15 to 20 m	926	5	2	8	9	1	7	1	8	48	2
Tree over 20 m	370	2	1	3	0	0	13	0	0	23	5